THE HAWAII GEOTHERMAL PROJECT

MODELLING OF A VOLCANIC ISLAND GEOTHERMAL RESERVOIR

September 1978

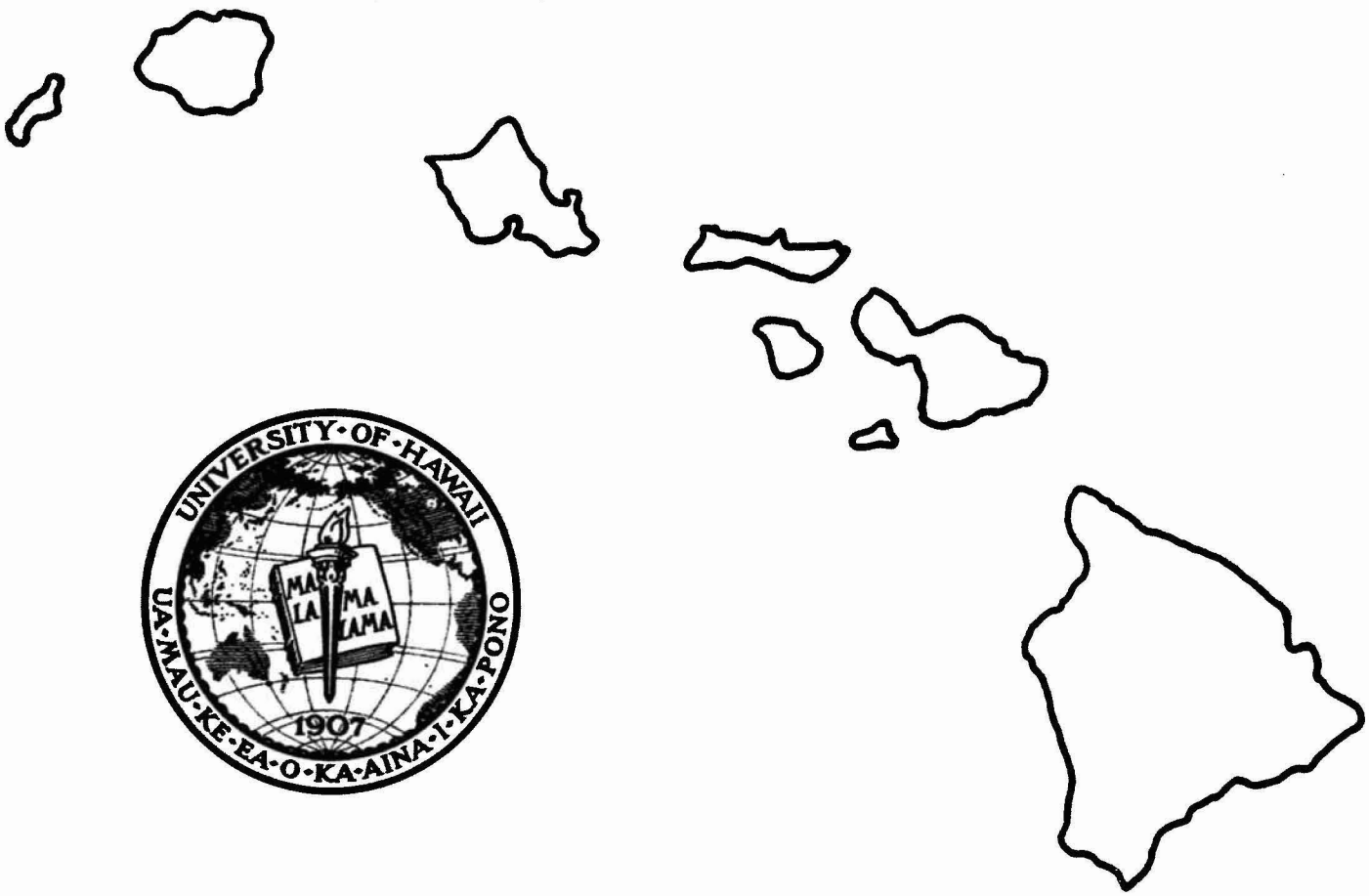

HAWAII GEOTHERMAL PROJECT

MODELLING OF A VOLCANIC ISLAND GEOTHERMAL RESERVOIR

September 1978

by

Ping Cheng

Kah Hie Lau

SUPPORT FOR PROJECT PROVIDED BY:

Department of Energy, Contract EY-76-C-03-1093
Energy Research and Development Administration, Contract E(04-3)-1093
National Science Foundation, Grant GI 38319
State of Hawaii, Grants RCUH 5774, 5784, 5942
County of Hawaii, Grant RCUH 5773
Hawaiian Electric Company, Grants RCUH 5809, 5828

University of Hawaii
Holmes Hall 206 2540 Dole Street
Honolulu, Hawaii 96822

ABSTRACT

Prior to the drilling of the HGP-A well at the Kapoho geothermal field in December 1975, it had generally been assumed that geothermal reservoirs on the Island of Hawaii were low-temperature liquid-dominated reservoirs which were constantly recharged from the ocean. Two numerical studies based on this conceptual model were carried out to investigate heat transfer and fluid flow characteristics in such a reservoir. It was found that (1) even under the most unfavorable conditions, i.e., in the absence of caprock for the prevention of heat loss and with constant recharge from cold seawater, it is possible to have a large amount of hot water at shallow depth, (2) the upwelling of the water table resulting from geothermal heating is small, and (3) the rate of contraction of isotherms resulting from the withdrawal of fluid from a production well depends not only on the withdrawal rate, but also on the size of the heat source as well as the relative location of the production well and the heat source.

After the drilling of the HGP-A well had been completed in April 1976, it was found from the core samples that the permeability of the formation varies with depth, and that the low salinity of the water samples taken from the well indicates that there is a barrier between the well and the ocean, preventing the free flow of seawater. Thus, a third numerical model taking into consideration the layered structure of the formation, with recharge and discharge through an upper permeable boundary, was carried out to simulate the free convection processes at the Kapoho geothermal field. In addition, analytical studies on convective heat transfer from dikes and sills in an aquifer with high permeability have been performed, and analytical expressions for heat transfer rates and the size of the hot water zone from hot intrusives have been obtained. The results of this investigation have given considerable insight on heat and mass transfer processes in a liquid-dominated volcanic geothermal reservoir.

TABLE OF CONTENTS

LIST OF FIGURES

LIST OF FIGURES (Continued)

INTRODUCTION

The task force for reservoir engineering consisting of the numerical modelling and well testing groups was formed during Phase I of the project. The initial assignment of the modelling group was to carry out numerical studies to assess whether a large amount of hot water exists in a volcanic island reservoir, unconfined from the top and constantly recharged with cold seawater. The ultimate objective of the modelling group was to develop a computer code capable of simulating the performance of a geothermal well in a liquid-dominated volcanic island reservoir. From a number of numerical models carried out during Phases I and II of the project, it was concluded that a large amount of hot water at high temperature is indeed possible in the Hawaiian island reservoir even under the most unfavorable conditions where a caprock is absent and with cold water being recharged from the ocean. During this period of time a number of analytical studies were also carried out on heat transfer from hot intrusives such as dikes and sills embedded in a formation with high permeability. After the HGP-A well had been drilled and field data analyzed, it was found in contrast with earlier speculation that (1) the permeability of the formation is small, (2) the low chloride content of water samples taken from the well suggests that there is a barrier between the well and the ocean to prevent the free flow of seawater, and (3) the bottomhole temperature and pressure measurements indicate that two-phase flow rather than single-phase flow exists in the formation. Since a meaningful simulation of the Kapoho geothermal field cannot be carried out until the reservoir characteristics are known, it was decided to discontinue the numerical modelling efforts until more holes in the area are drilled and well testing programs completed. The following is a summary of results obtained between May 1973 to September 1977 during which the numerical modelling work was funded. The results of the investigation have given considerable insight on heat and mass transfer processes in a liquid-dominated geothermal reservoir. Details of the work are reported in twenty publications[3-22].

OBJECTIVES

The primary objectives of this task have been (1) to assist in the assessment of geothermal resources on the island of Hawaii; (2) to estimate the capacity of the Kapoho geothermal field; (3) to predict the lifespan and performance of a geothermal well under different operating and resource conditions; and (4) to study the environmental impacts on the Ghyben-Herzberg lens resulting from withdrawal and reinjection of geothermal fluids.

NUMERICAL STUDIES

Prior to the drilling of the HGP-A well, it had generally been assumed that geothermal reservoirs on the Island of Hawaii are low-temperature hot-water reservoirs which are constantly recharged from the ocean, owing to the high porosity and permeability of the basaltic formation. It had been speculated that while aquifers at shallow depth on the island may be unconfined from the top, confined aquifers may exist at depth due to self-sealing effects. The heating of the groundwater in the aquifers is provided by a magma chamber at shallow depth, the rift zone, as well as numerous hot intrusives. An overly-simplified view of the Hawaii geothermal reservoir is shown in Fig. 1.

As the detailed geological and hydrological conditions at the Kapoho area were unknown prior to the drilling, the strategy adopted by the numerical simulation group had been to study simplified situations during the initial phase of the work. These simplified models, which consider different

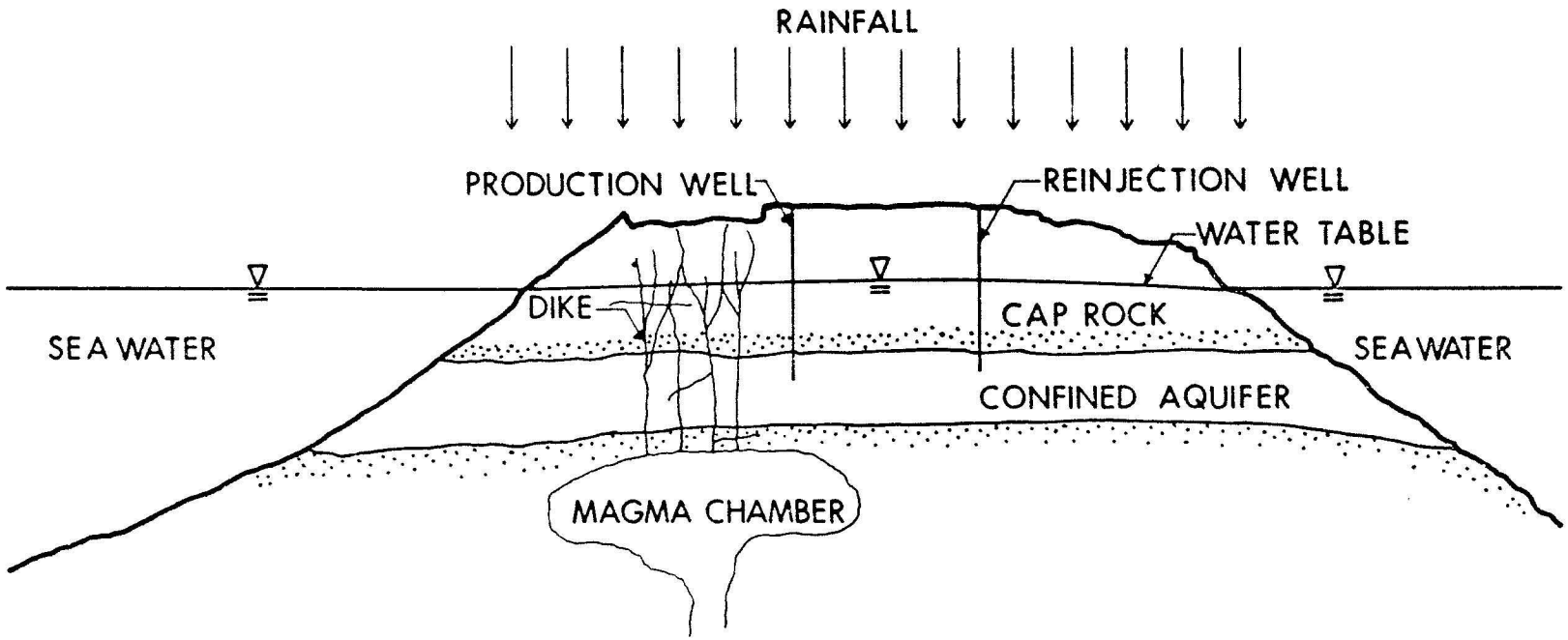

Figure 1. Island Aquifer with Geothermal Heat Source

effects one at a time, will aid in a qualitative understanding of the physical processes involved. After maturity and expertise have been developed and geophysical exploration data on the Kapoho area have been analyzed, more realistic models will be considered. The research work will then culminate in the development of a general computer code, capable of predicting the characteristics of the Kapoho geothermal field. For the initial models, the Hawaii geothermal reservoir (Fig. 1) is idealized as a two-dimensional porous medium, heated by impermeable bedrock from below, and recharged from the ocean through vertical boundaries (Fig. 2). To simplify the mathematical formulation of the problem, the following additional assumptions have been made:

A. The temperature of the fluid is everywhere below boiling for the pressure at that depth.

B. Properties of the groundwater and the rock formation such as the thermal conductivities, specific heats, kinematic viscosity, and permeability are assumed to be homogeneous and isotropic.

C. The Boussinesq approximation, used in classical free convection problems, is employed.

The mathematical model is based on the conservation laws of heat and mass, as well as the Darcy law for flow through a porous medium. With the above approximations, the governing equations in rectangular coordinates can be combined and reduced to the following two coupled non-linear partial differential equations in terms of P and θ as

$$\frac{\partial^2 P}{\partial X^2} + \frac{\partial^2 P}{\partial Z^2} = \varepsilon \frac{\partial \theta}{\partial Z} \quad , \tag{1}$$

$$D \left[- \frac{\partial P}{\partial X} \frac{\partial \theta}{\partial X} - \left(\frac{\partial P}{\partial X} + 1 - \varepsilon\theta \right) \frac{\partial \theta}{\partial Z} \right] + \frac{\partial \theta}{\partial \tau} = \frac{\partial^2 \theta}{\partial X^2} + \frac{\partial^2 \theta}{\partial Z^2} \quad , \tag{2}$$

where

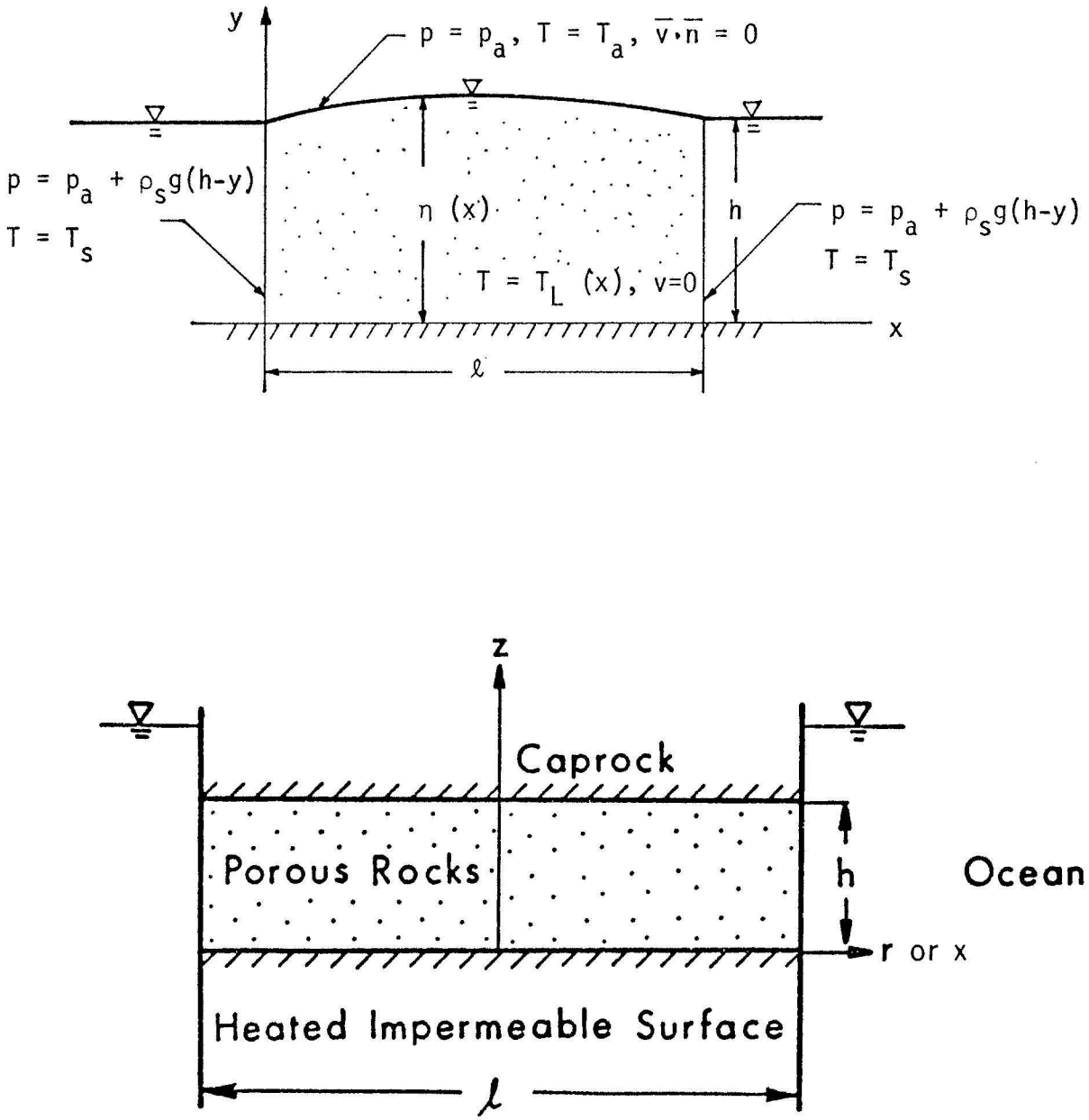

Figure 2. Reservoir Unconfined from the Top (upper figure) and Reservoir Confined from the Top (lower figure).

$$P \equiv \frac{p-p_o}{\rho_s gh} \quad , \quad \theta \equiv \frac{T-T_s}{T_m-T_s} \quad , \quad \tau \equiv \alpha t/\sigma h^2 \quad , \quad X \equiv x/h \quad , \quad Z \equiv z/h \quad ,$$

$$L \equiv \ell/h \quad , \quad \varepsilon \equiv \beta(T_m-T_s) \quad , \quad \text{and} \quad D \equiv \rho_s Kgh/\alpha\mu \quad ,$$

with p, T, t, ρ, β and μ denoting the pressure, temperature, time, density, thermal expansion coefficient, viscosity; α and K denoting the thermal diffusivity and permeability of the medium; g the gravitational acceleration; T_m denoting the maximum temperature of the impermeable surface, and the subscript "s" denoting the condition in the ocean; ε and D are dimensionless parameters; σ is the ratio of heat capacity of the fluid to that of the medium and p_o is some reference pressure which is assumed to be constant. In the above formulation, the parameters are D and ε which are related to the Rayleigh number by the relation $D\varepsilon = Ra$. If p_o is chosen to be the hydrostatic pressure which varies with depth, Eqs. (1a) and (2a) will be replaced by

$$\frac{\partial^2 P}{\partial X^2} + \frac{\partial^2 P}{\partial Z^2} = Ra \frac{\partial \theta}{\partial Z} \quad , \tag{3}$$

$$-\left[\frac{\partial P}{\partial X}\frac{\partial \theta}{\partial X} + \left(\frac{\partial P}{\partial Z} - Ra\theta\right)\frac{\partial \theta}{\partial Z}\right] + \frac{\partial \theta}{\partial \tau} = \frac{\partial^2 \theta}{\partial X^2} + \frac{\partial^2 \theta}{\partial Z^2} \quad , \tag{4}$$

where Ra is the only parameter of the problem.

For most of the two-dimensional problems of free convection in geothermal reservoirs, it is convenient to express the governing equations in terms of stream function and temperature which are given by

$$\frac{\partial^2 \Psi}{\partial X^2} + \frac{\partial^2 \Psi}{\partial Z^2} = -\frac{\partial \theta}{\partial X} \quad , \tag{5}$$

$$\frac{\partial^2 \theta}{\partial X^2} + \frac{\partial^2 \theta}{\partial Z^2} = Ra\left(\frac{\partial \Psi}{\partial Y}\frac{\partial \theta}{\partial X} - \frac{\partial \Psi}{\partial X}\frac{\partial \theta}{\partial Y}\right) + \frac{\partial \theta}{\partial \tau} \quad , \tag{6}$$

where $\Psi \equiv \mu\psi/\rho_s gh\beta(T_m-T_s)K$ which is related to the dimensionless velocity components by $U = \partial\Psi/\partial Z$ and $V = -\partial\Psi/\partial X$. With appropriate boundary and initial conditions, Eqs. (1) and (2) [or the equivalent set of equations (3) - (14) or (5) - (6)] have been solved numerically for the investigation of the following problems.

Model No. 1 Convection in a Geothermal Reservoir Unconfined from the Top [3.4]

To study the possibility of the upwelling of the water table due to geothermal heating as suggested by Keller (1), the problem of steady free convection in an unconfined geothermal reservoir was treated (Fig. 2a). In the mathematical formulation of the problem, the shape of the water table is not known a priori and must be determined from the solution. Since exact numerical solutions to the problem are very difficult, approximate perturbation solutions applicable to reservoirs at low Rayleigh numbers are obtained. As a result of these approximations, the governing equations are linearized and the zero-order and the first-order problems are, respectively, the Laplace equation and Poission equation with nonhomogeneous boundary conditions, which can be solved numerically. Figure 3 shows the isotherms in an unconfined geothermal reservoir with D = 500 and ε = 0.1, or Ra = 50, where Case A represents heating due to a vertical hot dike, 0.5 unit in height and 2 units in width, located at the center of the aquifer with a cold impermeable surface at the bottom; Case B represents heating due to a magma chamber from below. Heating in Case C is due to the combination of a dike as in Case A, and a heated horizontal bedrock as in Case B. The effects of different heat sources on the upwelling of the water table are shown in Fig. 4, where it can be concluded that the upwelling of water table due to geothermal heating is small.

Model No. 2 Convection in a Geothermal Reservoir Confined from the Top

The second model considered is that of a two-dimensional reservoir confined by caprock at the top and bedrock at the bottom with recharge through vertical boundaries from the ocean (see Fig. 2b). Since no free surfaces are involved in this problem, exact numerical solutions for any Rayleigh number can be obtained by finite difference methods. This model was used to study the formation and withdrawal of fluids in an island geothermal reservoir.

(A) Formation of an Island Geothermal Reservoir [9]

Consider that the idealized aquifer as shown in Fig. 2b having an aspect ratio of 4, initially isothermal and motionless, is suddenly heated by an intruded magma chamber at a shallow depth. The subsequent development of isotherms in the

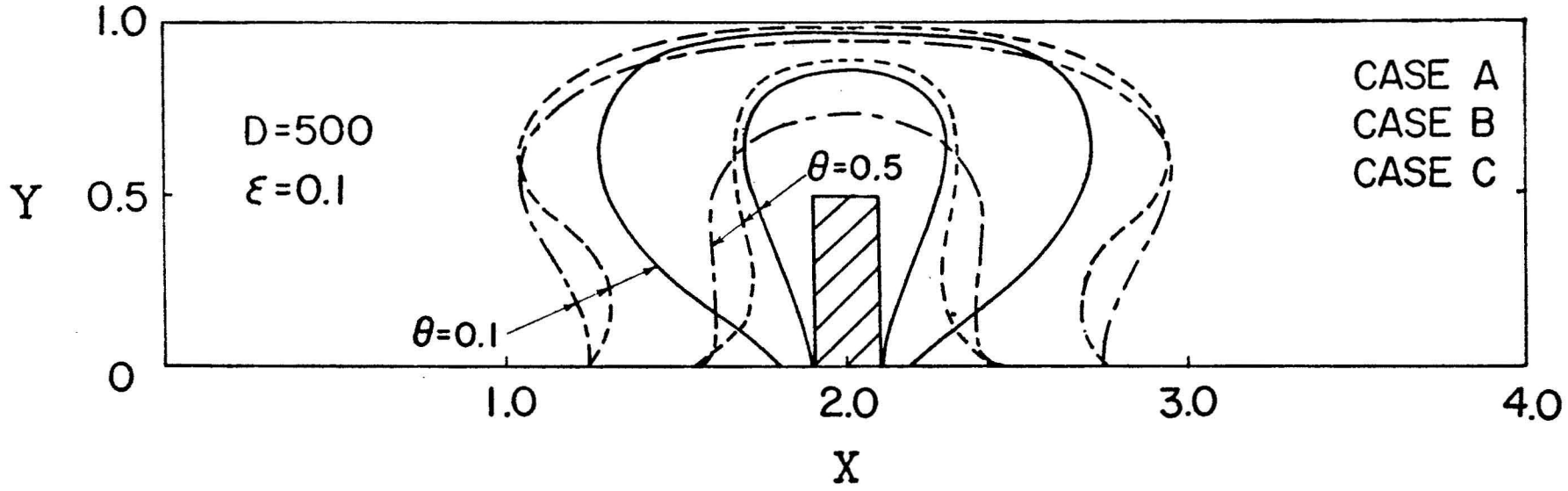

Figure 3. Effects of Vertical and Horizontal Heating on Temperature Contours in an Unconfined Geothermal Reservoir

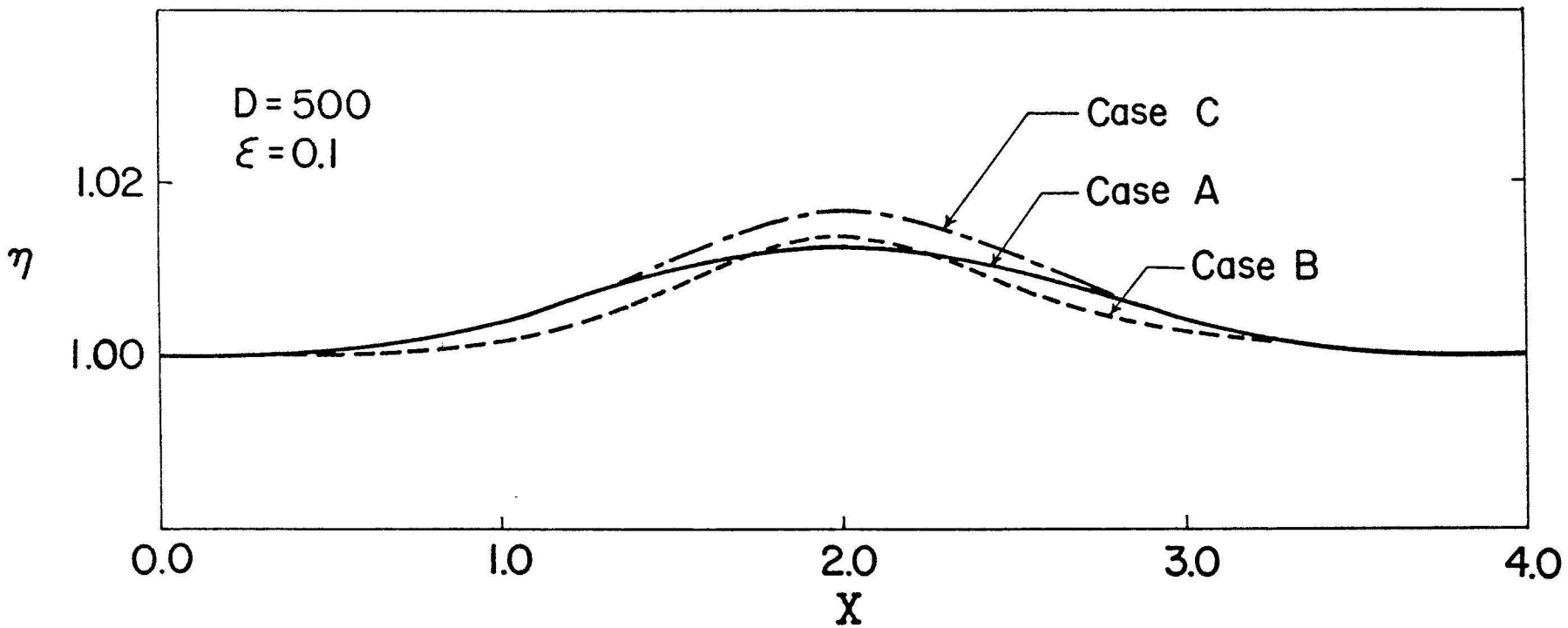

Figure 4. Effects of Heat Sources on the Upwelling of Water Table for Cases A, B, and C

reservoir having D = 4,000 and ε = .05 (ra = 200) is shown in Fig. 5 where τ = 0.001 corresponds to 200 years on the real time scale. It is shown in the figure that the isotherms move gradually upward and reach a steady state condition approximately at τ= 0.035, corresponding to approximately 7000 years. It is found that the time required to reach steady state increases as the value of D decreases.

Effects of Rayleigh Number [5]

Figures 6-8 show the steady state convection pattern and isotherms in an axisymmetric reservoir at different values of Ra. As shown in Figs. 6a and 6b, cold water from the ocean moves inland along the lower portion of the aquifer and is gradually being heated by the hot bedrock. Near the point of maximum heating, the fluid rises as a thermal plume. As the hot water reaches the top, it spreads around the caprock and is finally discharged to the ocean in the upper portion of the aquifer. A comparison of Figs. 6a and 6b shows that close convective cells disappear as the value of Ra is increased. The effect of Ra on the isotherms is shown in Fig. 7. It shows that for small values of Ra (Ra = 50 for example), the shapes of the isotherms are similar to those by heat conduction. As the values of Ra increase, the isotherms develop into mushroom shapes. The results have important implications on the selection of a drilling site. They indicate that for a reservoir with large value of Ra and having a hot heat source from below, a large amount of hot water is indeed available at shallow depths. Fig. 8 shows the vertical temperature profiles at different locations in an island aquifer. The dimensionless temperatures at the center line of the thermal plume increase rapidly from nearly zero at the caprock to almost unity somewhat below the caprock. The vertical temperature profiles along the thermal plume are shown to be different from the rest of the profiles which have a temperature reversal at a lower elevation. It is worth mentioning that the temperature reversal occurs because of the lateral movement of groundwater. It is interesting to note that temperature vs. depth measurements obtained by Keller [1] show also a temperature reversal behavior (Fig. 9). A comparison between theory and masurements shows a striking similarity (Fig. 10).

Effects of Thermal Boundary Condition at the Caprock [5]. Figure 11 shows the steady temperature distribution in a geothermal reservoir with an adiabatic caprock. The effects of thermal boundary condition on the caprock can be shown by comparing the isotherms in Fig. 11 to those of Fig. 7 which is for a reservoir

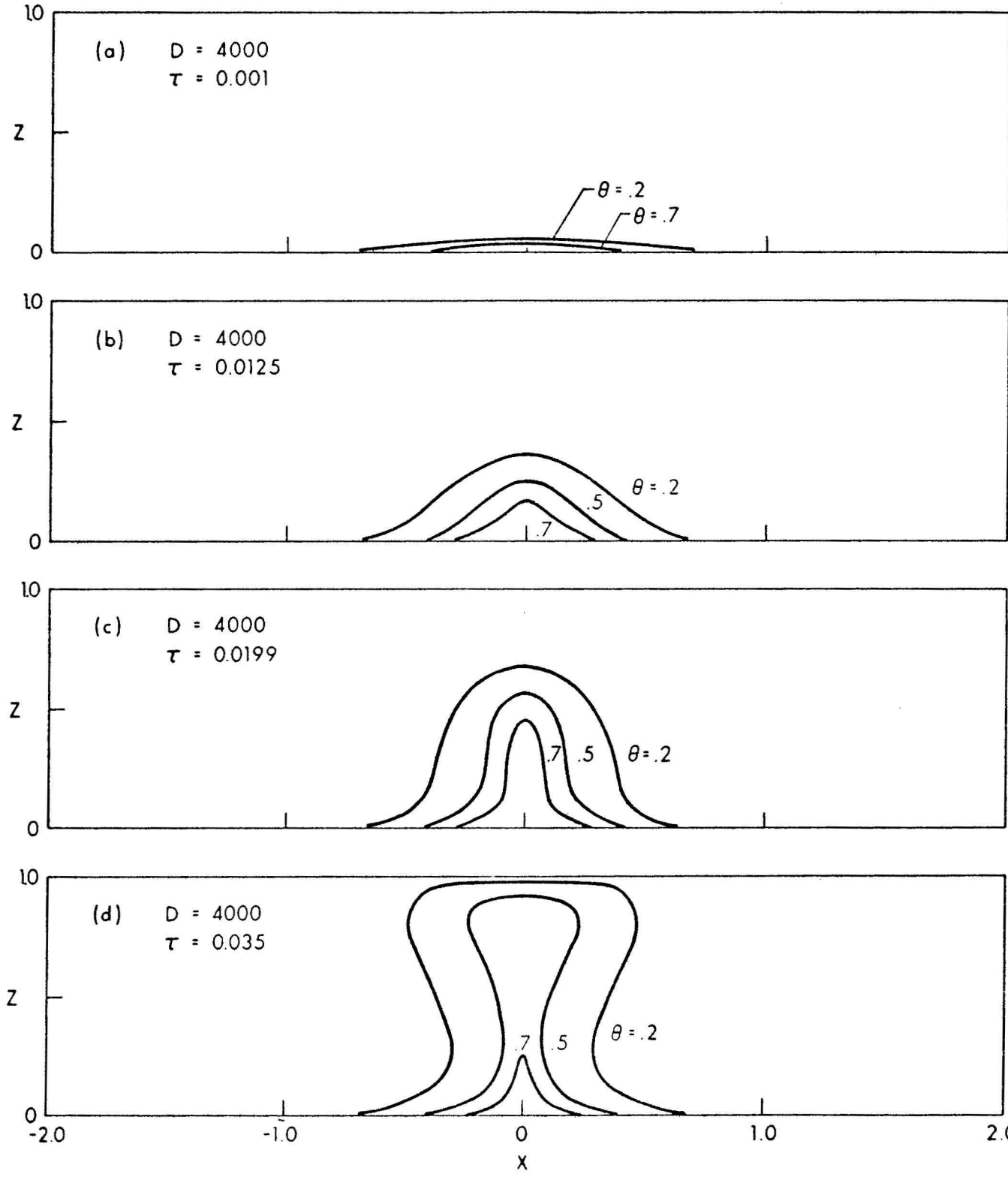

Figure 5. Development of Isotherms in a Capped Geothermal Reservoir at D = 4000 and ε = .05

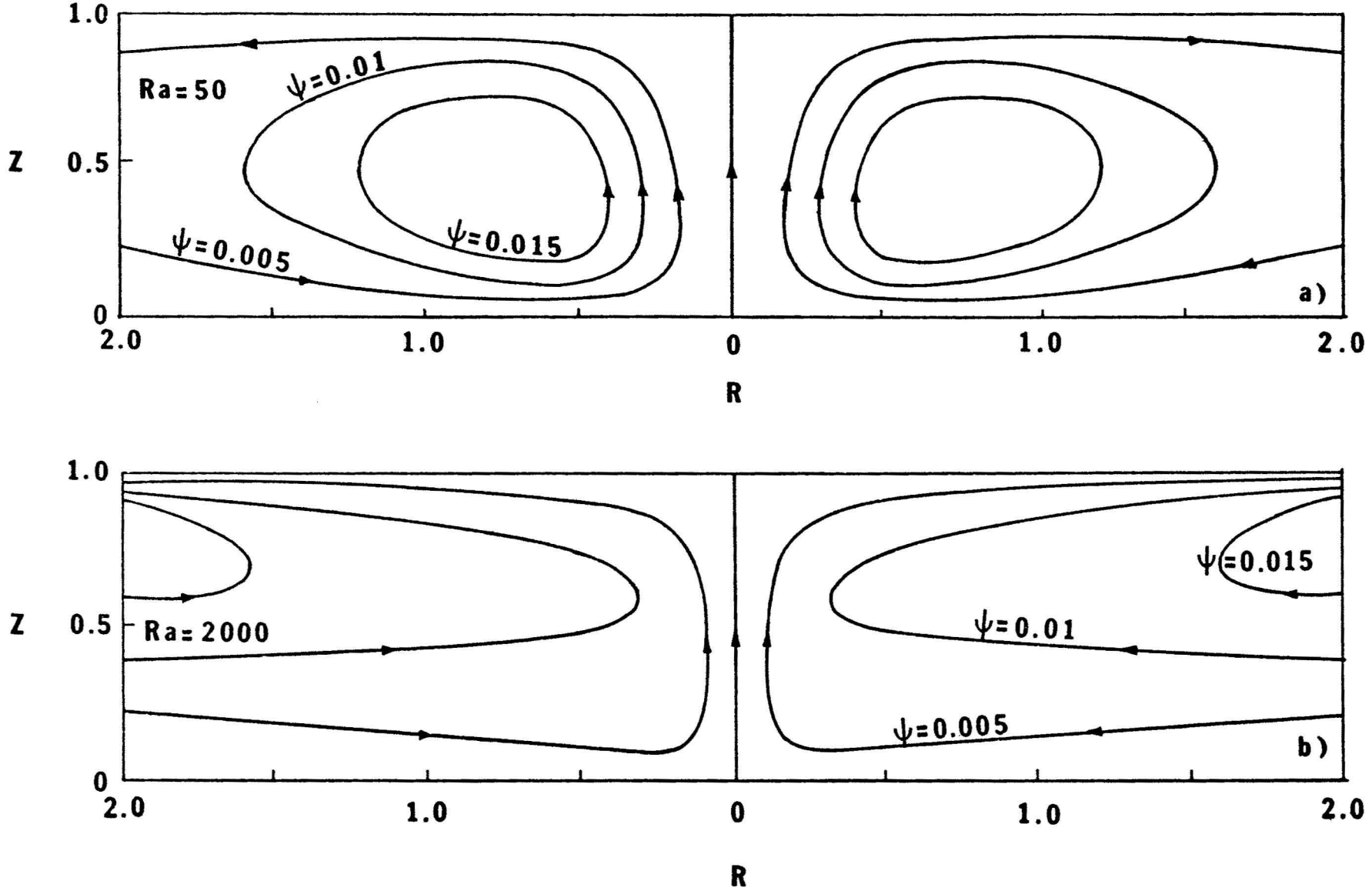

Figure 6. Streamlines for a Cylindrical Island Aquifer

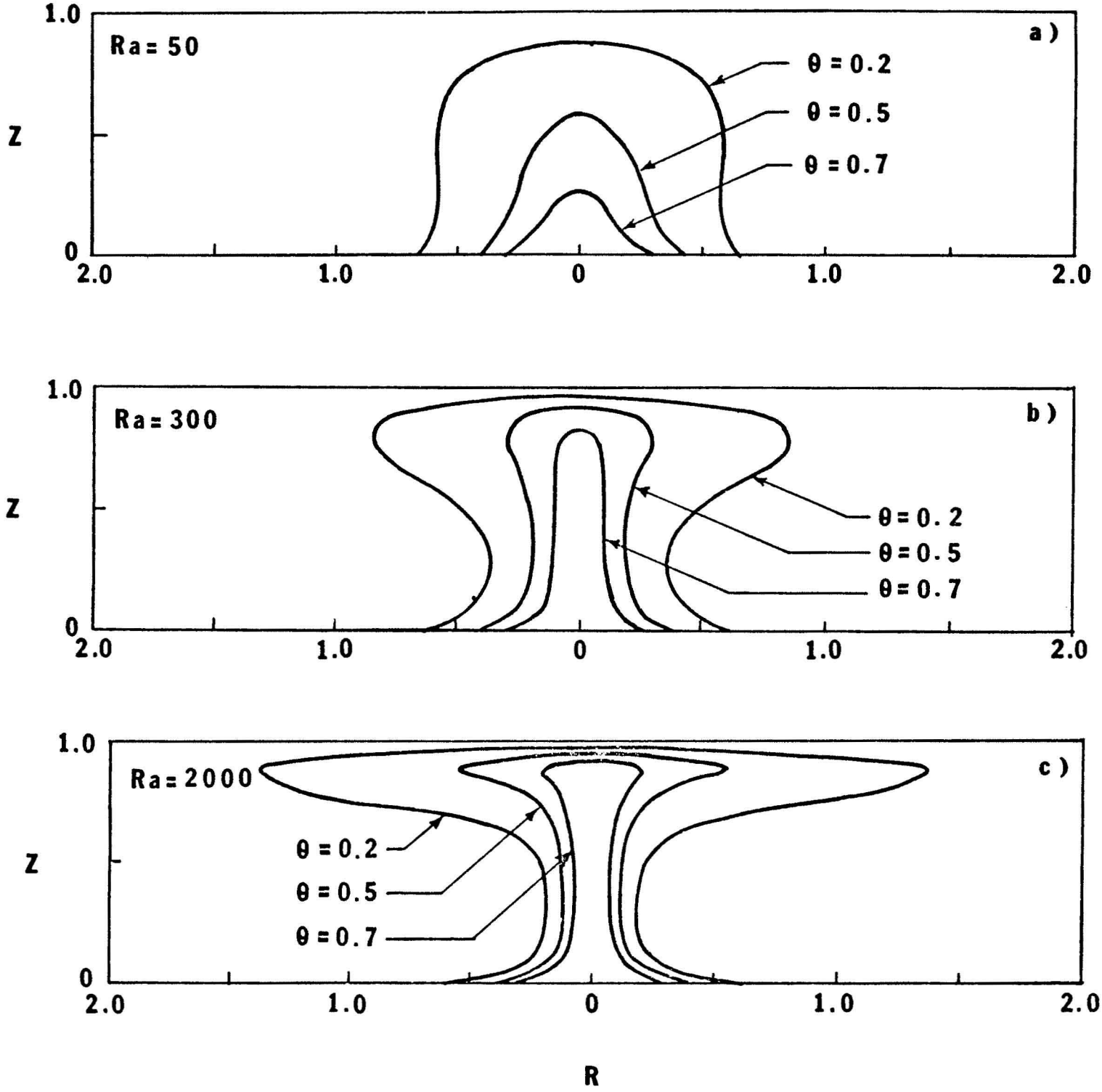

Figure 7. Temperature Contours in a Cylindrical Island Aquifer with Caprock Temperature Specified

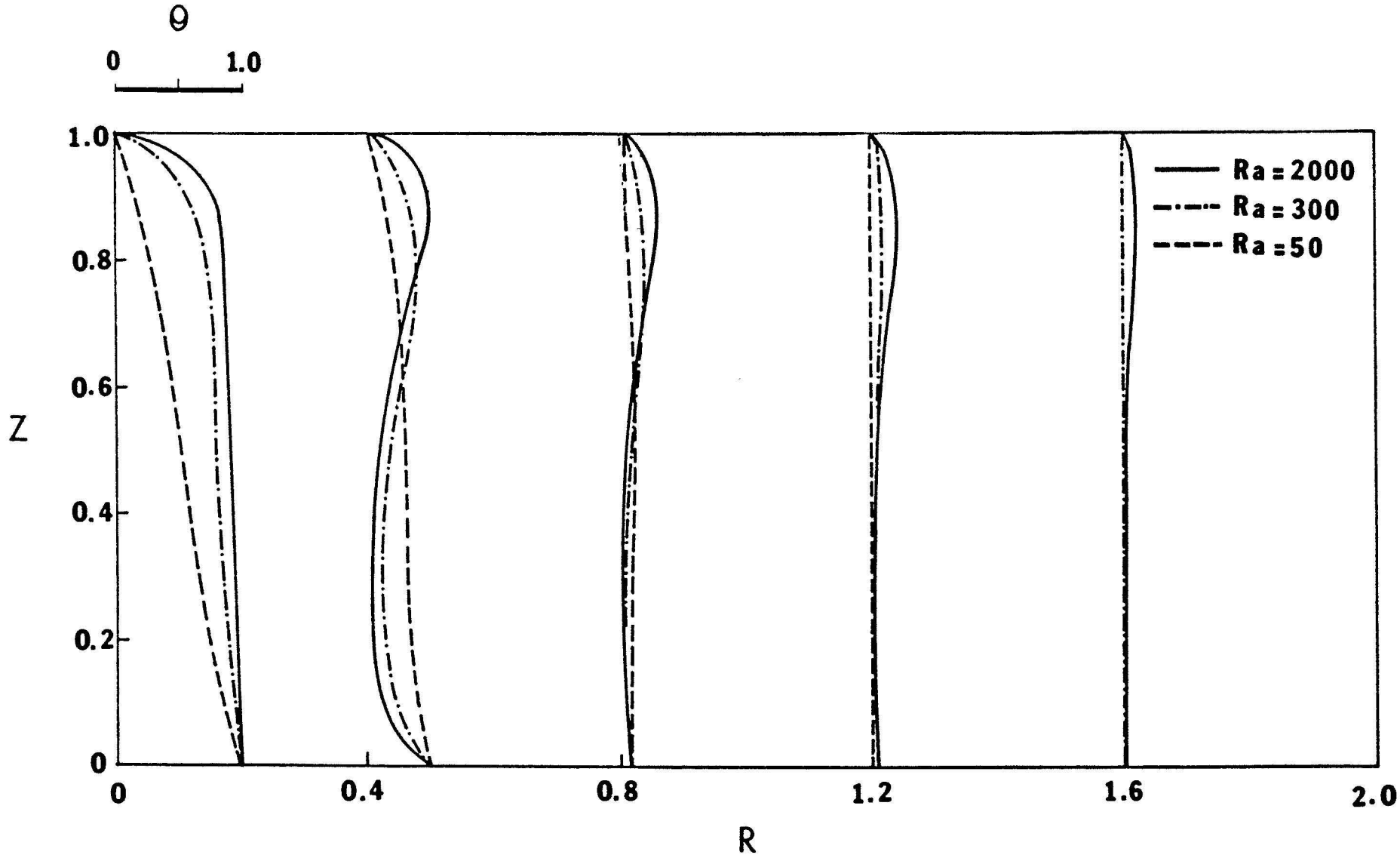

Figure 8. Vertical Temperature Profiles in a Cylindrical Island Aquifer with Caprock Temperature Specified

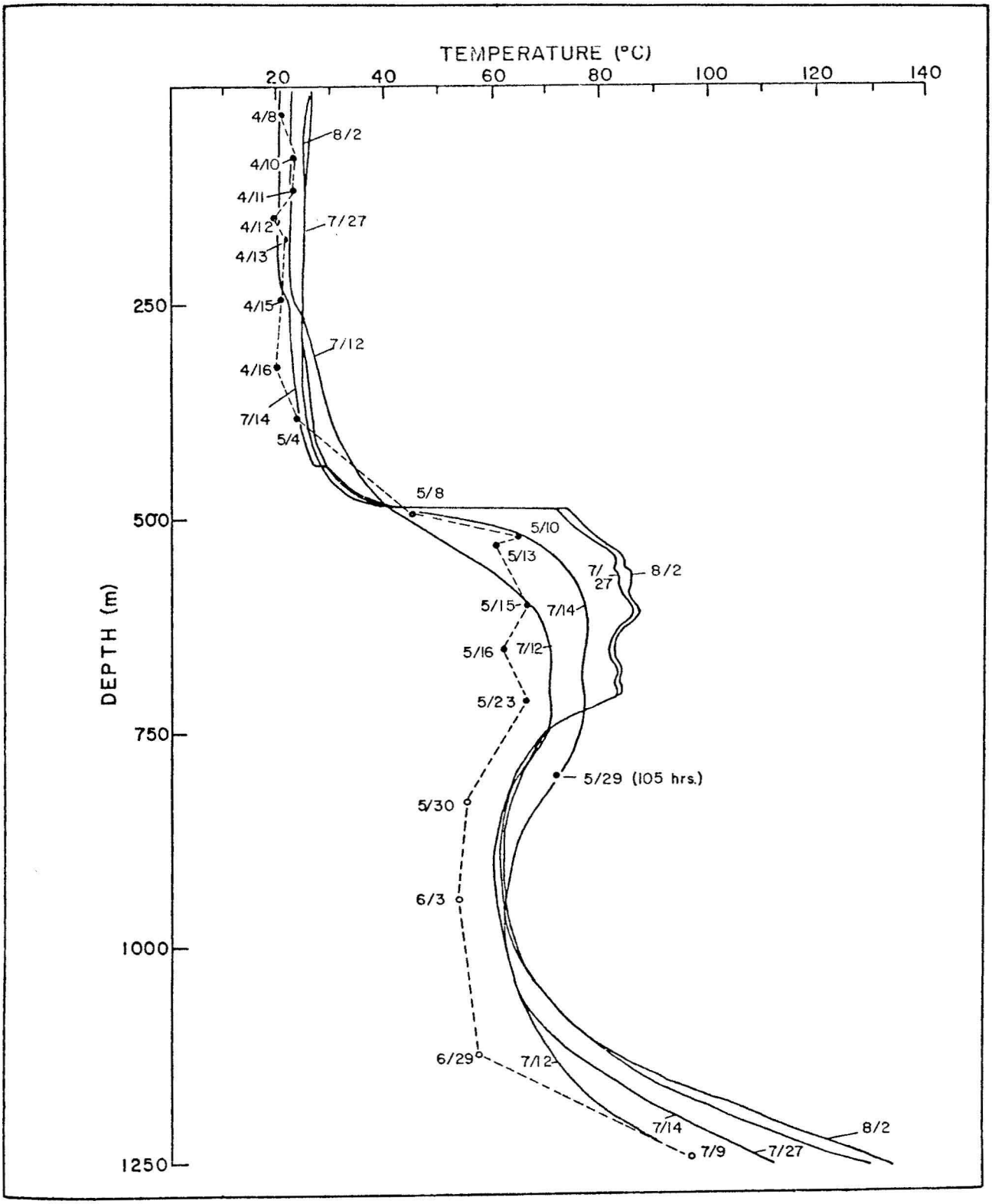

Figure 9. Temperature Profiles in the Kilauea Drill Hole Measured by Keller

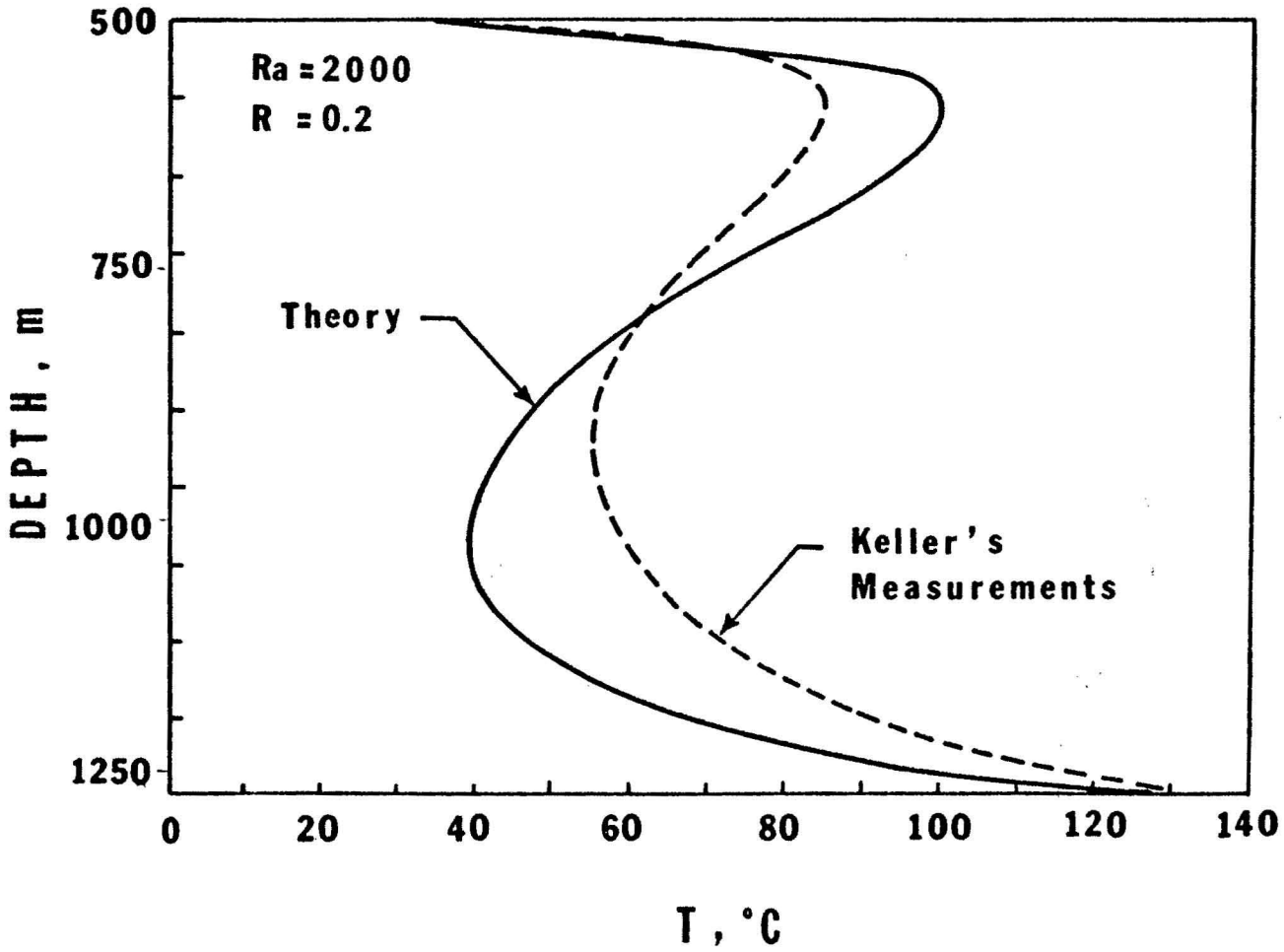

Figure 10. Comparison of Theory and Measurements

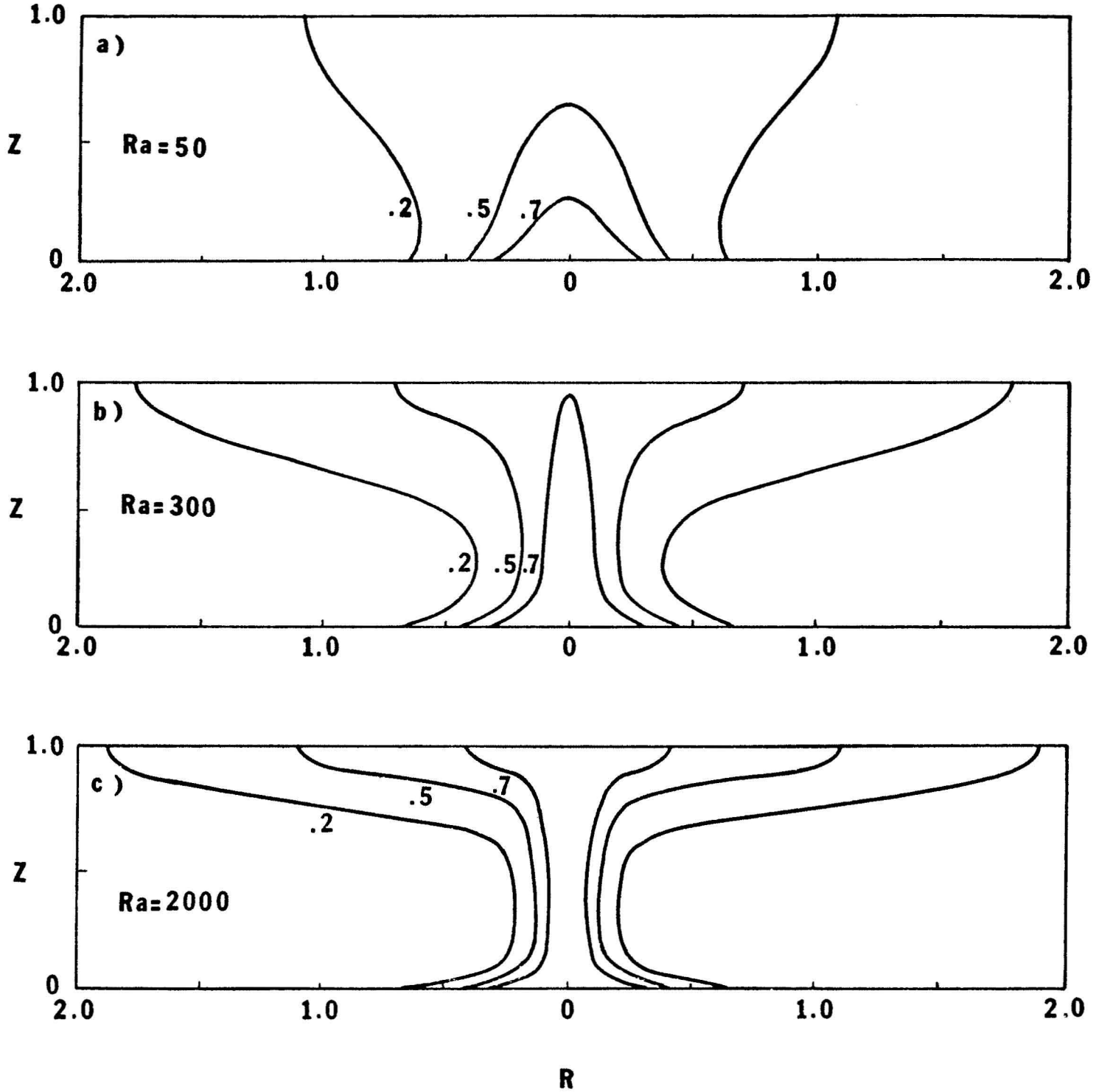

Figure 11. Temperature Contours in a Cylindrical Island Aquifer with Adiabatic Caprock

with a heat-conducting caprock. As expected, temperature distribution everywhere in the reservoir having adiabatic caprock is higher than that with a heat-conducting caprock. However, the increase in temperature is most significant in the region adjacent to the caprock. The larger the value of Ra, the smaller the region in which temperature is affected. In other words, for large values of Ra, the effect of thermal boundary condition on the caprock is confined to a small region adjacent to the caprock, with the temperature distribution in the rest of the reservoir remaining unaffected. Thus, the size of hot water zone at shallow depth depends on the thermal condition of the caprock. The effect of thermal boundary condition at the caprock on the total heat transfer rate of the bedrock is presented in Fig. 12, where it is shown that the heat transfer is relatively independent of the thermal boundary condition at the caprock.

Effects of Heating Length and Dike Intrusion [5]. The effects of heating length of the bedrock on steady state convection pattern and its associated isotherms are shown in Figs. 13 and 14. The number of convective cells and the associated thermal plumes are dependent upon the value of f, that is, the ratio of the heating length to the height of the reservoir. It is shown that two convective cells are generated for $f = 2$, while four convective cells are generated for $f = 3$. The effects of dike intrusion on convection pattern and temperature distribution are shown in Figs. 13c and 14c. Comparison of curves in Figs. 13 and 14 respectively shows that the convective pattern and the shape of isotherms depend not only on the size of the heating length but also on the manner it is heated, i.e., whether it is heated vertically or horizontally. For example, although Figs. 13b and 13c have the same heating length, the convective patterns and their associated temperature contours (as shown in Figs. 14b and 14c) are completely different.

(B) Withdrawal of Fluids in an Island Geothermal Reservoir [6, 8, 9]

Pressure gradients in a geothermal field can be generated by man-made withdrawal or reinjection of fluids during production. As a result, the convective movement of groundwater in the geothermal reservoir depends not only on the buoyancy force but also on the induced pressure gradients. For a sufficiently strong withdrawal rate, isotherms in the reservoir may contract which will have important implications to the lifespan of a geothermal well.

Figure 15 shows the contraction of isotherms of a rectangular geothermal reservoir with an aspect ratio of 4 and with $D = 7000$ and $\varepsilon = 0.05$ (or $Ra = 350$)

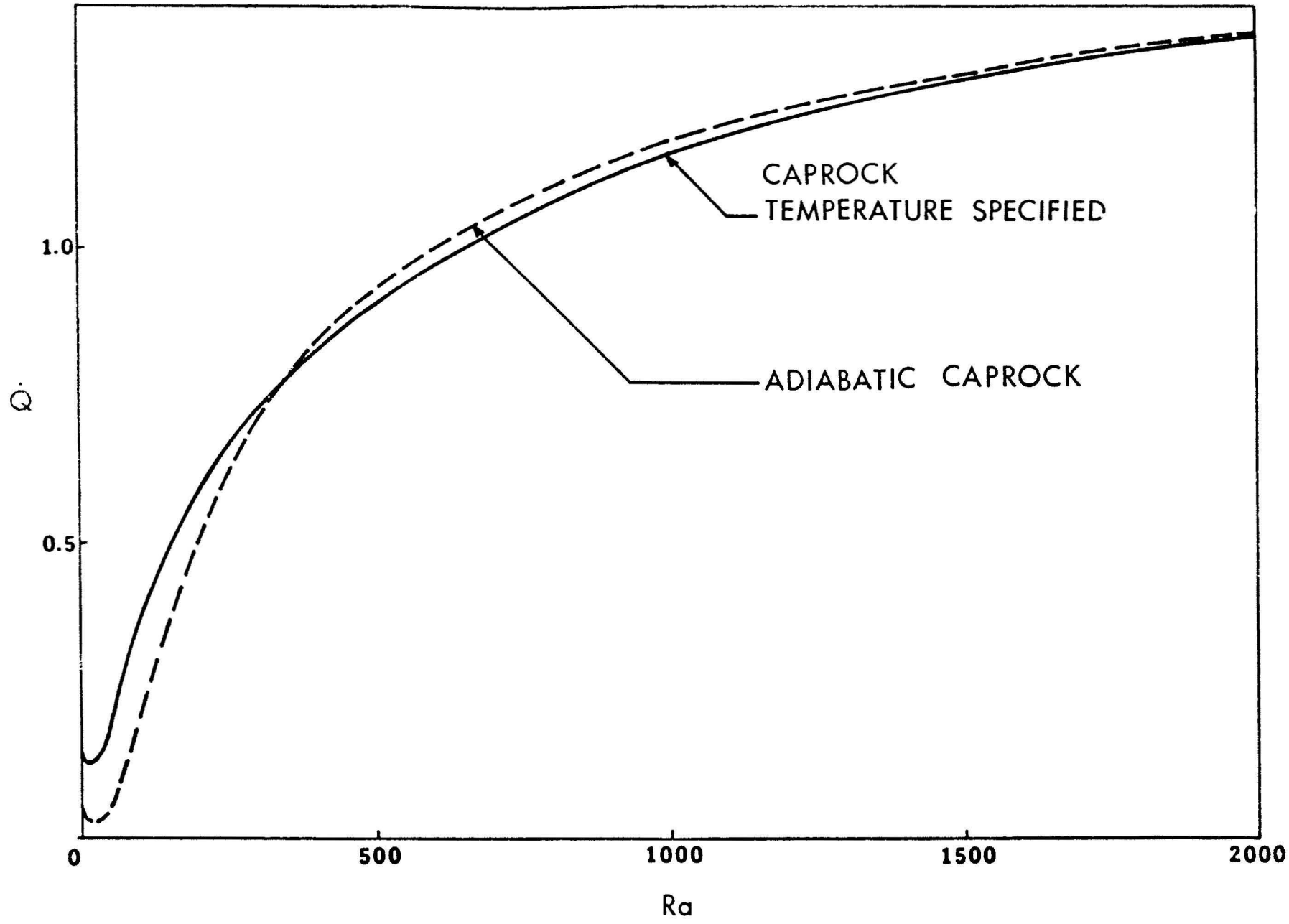

Figure 12. Effect of Thermal Boundary Condition of Caprock on Surface Heat Transfer Rate of the Bedrock

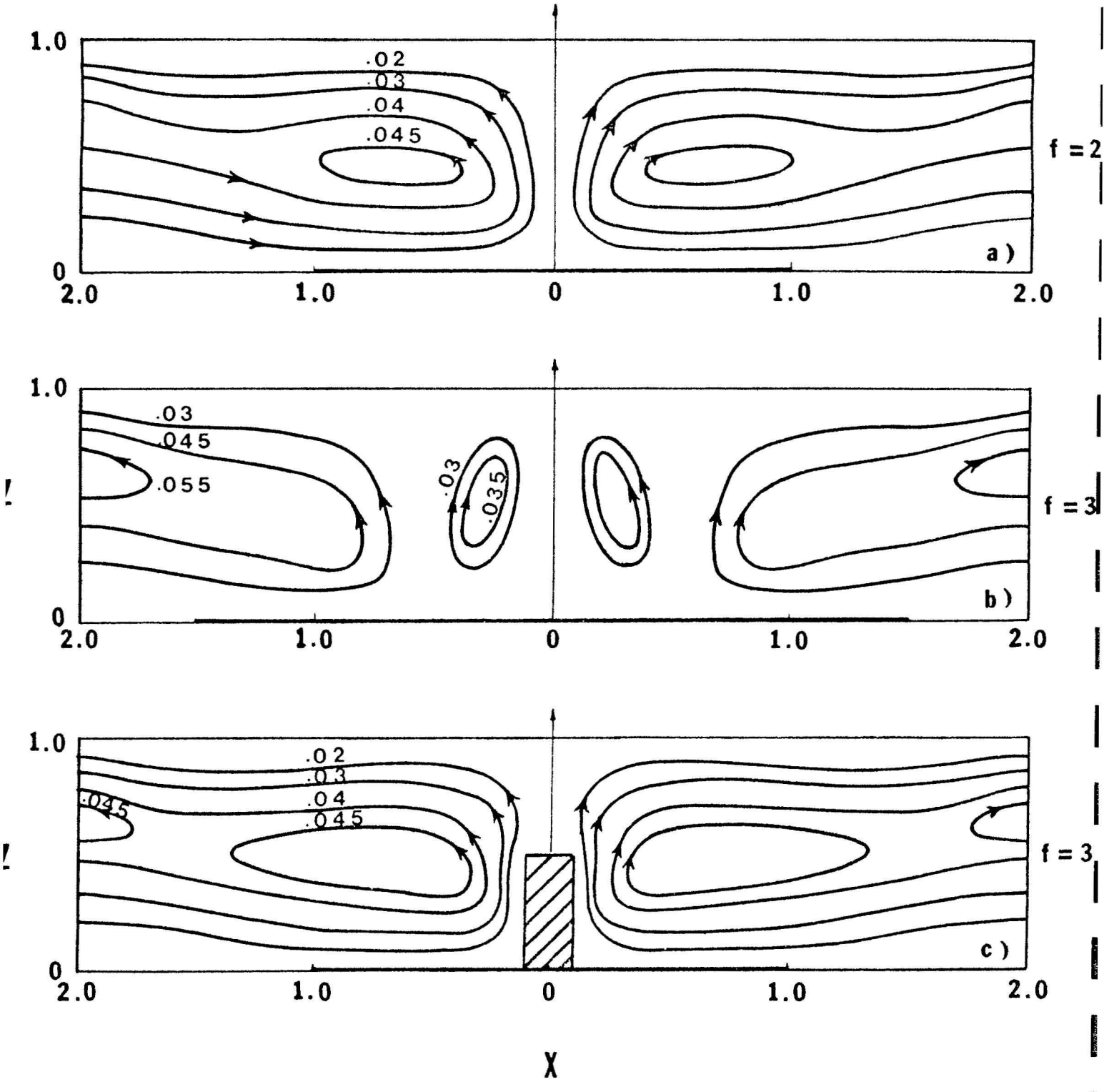

Figure 13. The Effects of Heating Length and Magmatic Intrusion on Streamlines in a Rectangular Reservoir with Heat-Conducting Caprocks

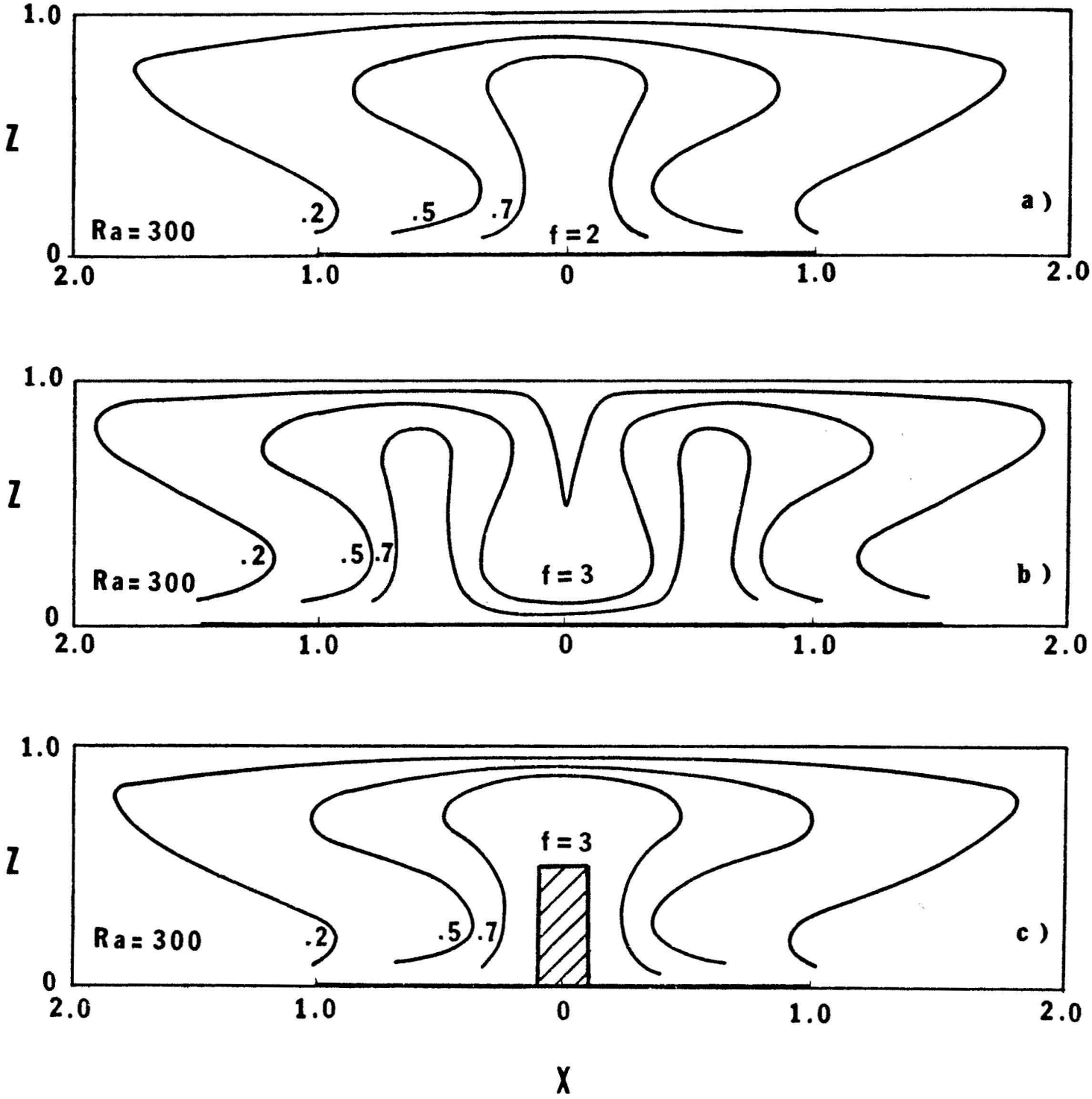

Figure 14. The Effects of Heating Length and Magmatic Intrusion on the Isotherms in a Rectangular Reservoir with Heat-Conducting Caprocks

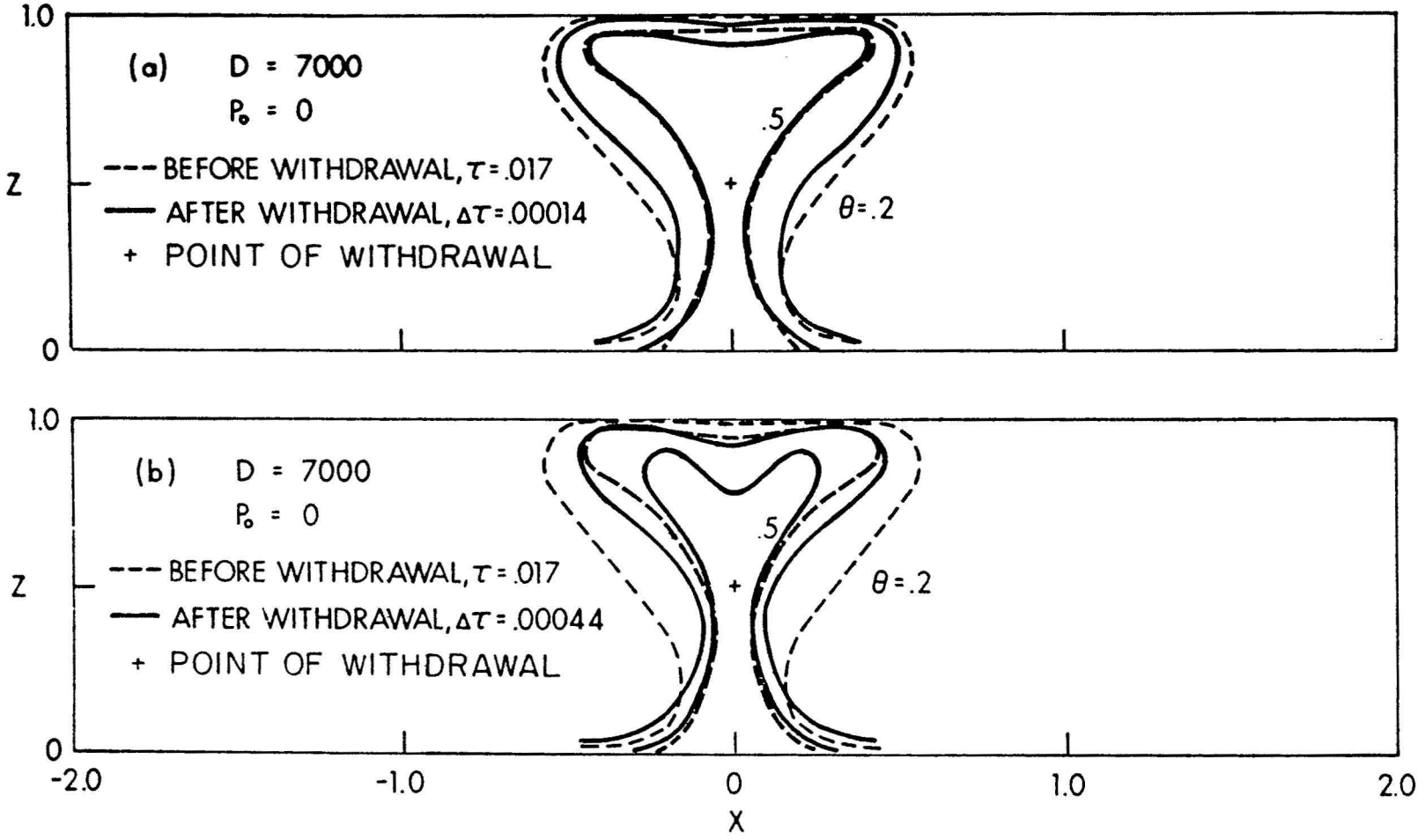

Figure 15. Contraction of Isotherms in a Geothermal Reservoir Resulting from Withdrawal of Fluids from a Point Sink

resulting from the fluid withdrawal. The dashed lines indicate the isotherms before fluid withdrawal, while the solid lines indicate the isotherms after 30 years (Fig. 15a) and 100 years (Fig. 15b) of continuous withdrawal of fluids at a rate of $7 \times 10^6 lb_m$/hr-ft from a point sink located at X = 0 and Z = 0.5, i.e., directly above the point of maximum heating. While it is shown in the figure that isotherms hardly change after 30 years of operation, the temperature of the groundwater above the sink decreases noticeably after 100 years of operation.

Figure 16 shows the contraction of isotherms resulting from the withdrawal of fluid along a line sink located vertically upward from the point (0, 0.5) to the top of the aquifer having D = 7000 and $\varepsilon = 0.05$. The isotherms before the fluid withdrawal are the same as those in Fig. 15 and are shown by dashed lines. The solid lines are the isotherms after 30 years of continuous withdrawal of fluids at the rate of $1.7 \times 10^7 lb_m$/hr-ft. At this rate of withdrawal, it is shown that the temperature of groundwater in the upper portion of the reservoir decreases noticeably after 30 years of operation. It should be noted that the rate of contraction of isotherms not only depends on the withdrawal rate but also on the size of the heating length, i.e., the temperature distribution of the bedrock.

Model No. 3. Convection in a Multi-Layered Geothermal Reservoir

Model No. 3 was developed after HGP-A well had been drilled. Preliminary analysis of data from geophysical exploration and well testing suggested that some of the assumptions made in the earlier models do not correspond to the conditions that exist at the Kapoho geothermal field. From the examination of mud loss during drilling and from core samples taken from the well, it appears that layered structure exists in the rock formation, and that there is no evidence of a caprock being formed. Analysis of the water samples taken from the well shows that the groundwater has an extremely low salinity, indicating that the groundwater is most likely to be of meteoric origin with little recharge from the ocean.

Model No. 3 assumes that (1) the aquifer can be recharged or discharged from the top through a permeable upper boundary, and (2) the aquifer is comprised of three layers with the middle layer being the least permeable, and the upper and lower layers being high and moderate in permeability. The heating of the groundwater in the aquifer is provided by dike complexes from the sides and a magma chamber from below. Since the three layers have different physical properties, the governing equations must be applied separately to the three layers. The boundary conditions at the interfaces are such that temperatures and stream functions are continuous and that flow rates normal to the interfaces are the same.

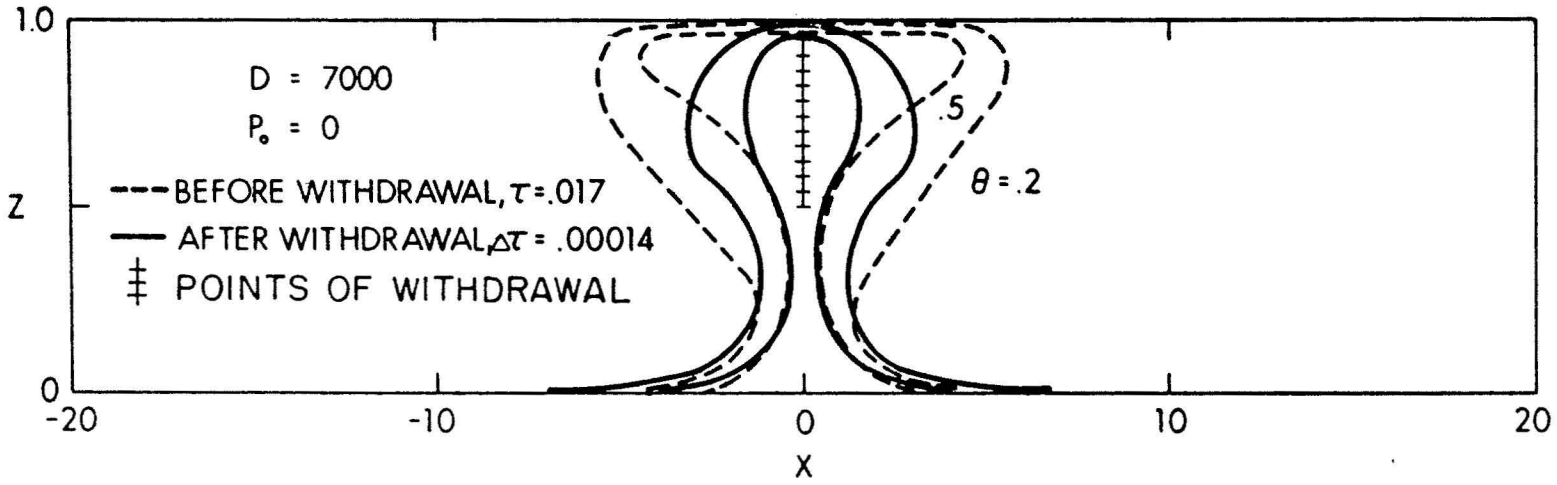

Figure 16. Contraction of Isotherms in a Geothermal Reservoir Resulting from Withdrawal of Fluids from a Line Sink

Numerical solutions have been carried out for six cases with different Rayleigh numbers and aspect (length to height) ratios. Representative results for streamlines and temperature distribution are shown in Fig. 17, where the aspect ratio is 2 and the Rayleigh numbers for the three layers are taken to be 300, 120 and 750. The multi-cellular flow with cell width of 0.5, plotted in Fig. 17a for half the domain, seems to be the preferred mode as the system approaches steady state. The streamlines in Fig. 17b show strong convective flows in the upper and lower layers where the permeabilities are higher. Cellular convection is absent in the middle layer where permeability is low. Vertical temperature profiles for this case are plotted in Fig. 18. Comparison of Fig. 18 with temperature profiles observed at HGP-A well (Fig. 19) shows a strong resemblance, demonstrating the credibility of the mathematical model.

ANALYTICAL STUDIES

It will be of great interest if some simple algebraic equations can be obtained for the calculations of heat transfer rate and size of the hot water zone adjacent to the hot intrusives which exist in the Kapoho geothermal field. For these purposes, some effort has been devoted to obtain analytical solutions for convective heat transfer from vertical or horizontal heated surfaces embedded in a rock formulation saturated with water. The methodology used to solve Eqs. (1) and (2) (or an equivalent set of equations) approximately is akin to the boundary layer simplifications in classical viscous flow theory. The following analytical solutions have been obtained.

Free Convection from a Dike.

Closed-form solutions have been obtained for steady free convection from an isothermal dike at T_w, trapped in a rock formation at T_∞. The expression for the size of the hot-water zone (i.e., the so-called thermal boundary layer thickness) is

$$\frac{\delta_T}{x} = \frac{6.31}{(Ra_x)^{1/2}} \quad , \tag{7}$$

where x is the coordinate along the surface of the dike. The local surface heat flux is

$$q = 0.444\ k\ A^{3/2} \left(\frac{\rho_\infty \beta g K}{\mu \alpha}\right)^{1/2} \times (3\lambda-1)/2 \quad , \tag{8}$$

where $A = T_w - T_\infty$.

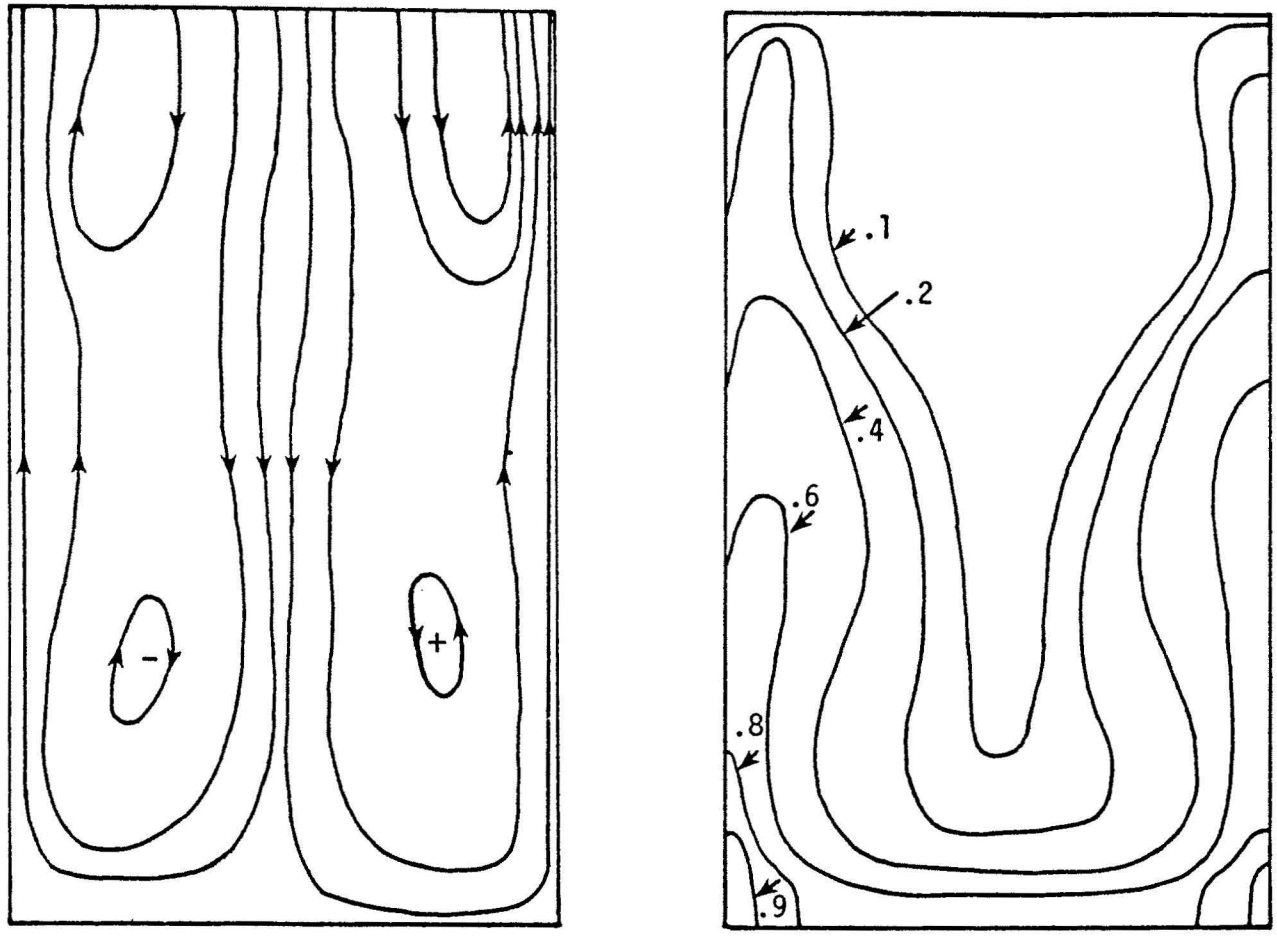

Figure 17. Steady State Stream Functions (Left) and Temperature Contours (Right)

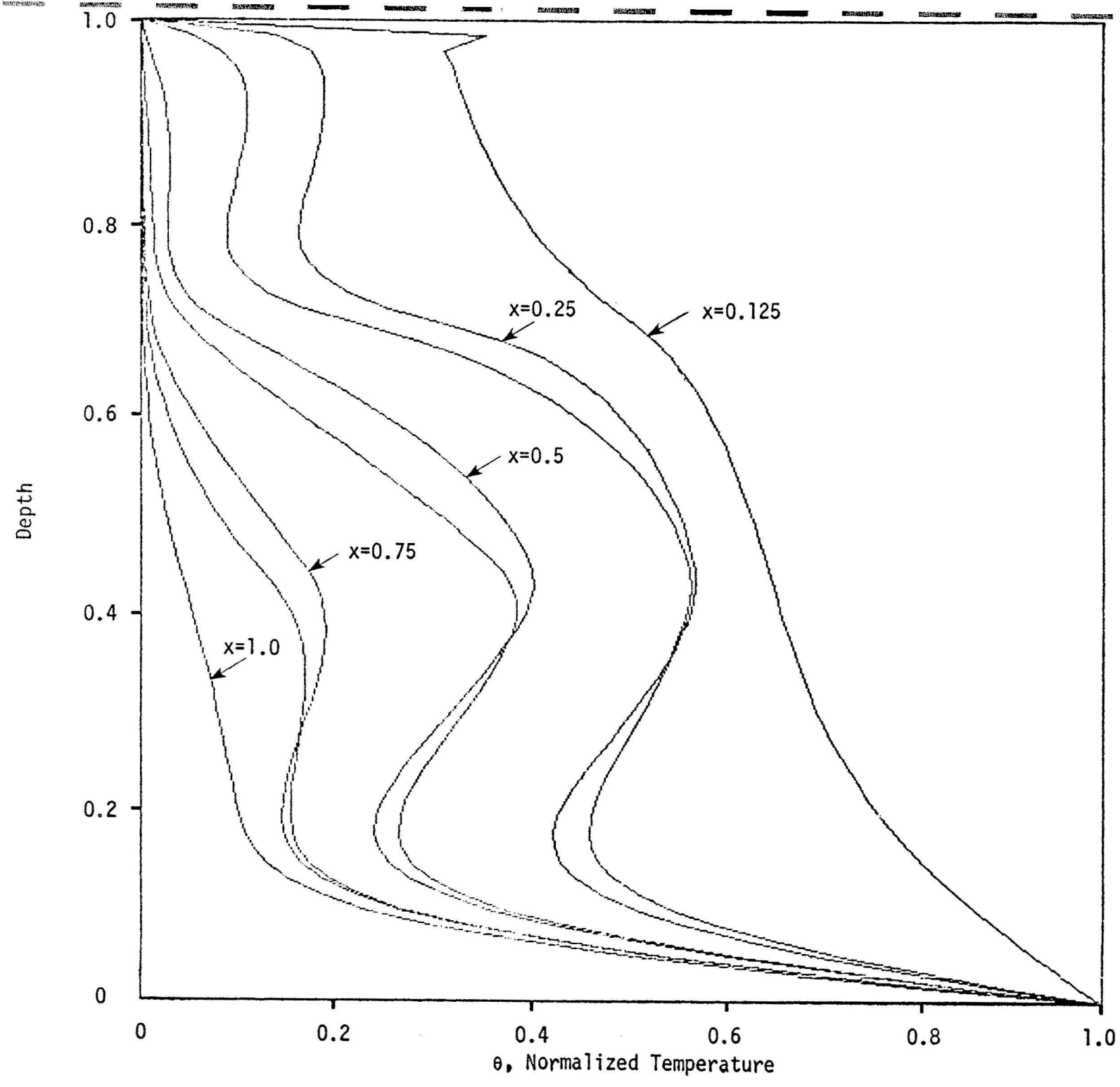
1.0
0.8
0.6
0.4
0.2
0
Depth
x=0.25
x=0.125
x=0.5
x=0.75
x=1.0
0
0.2
0.4
0.6
0.8
1.0
θ, Normalized Temperature

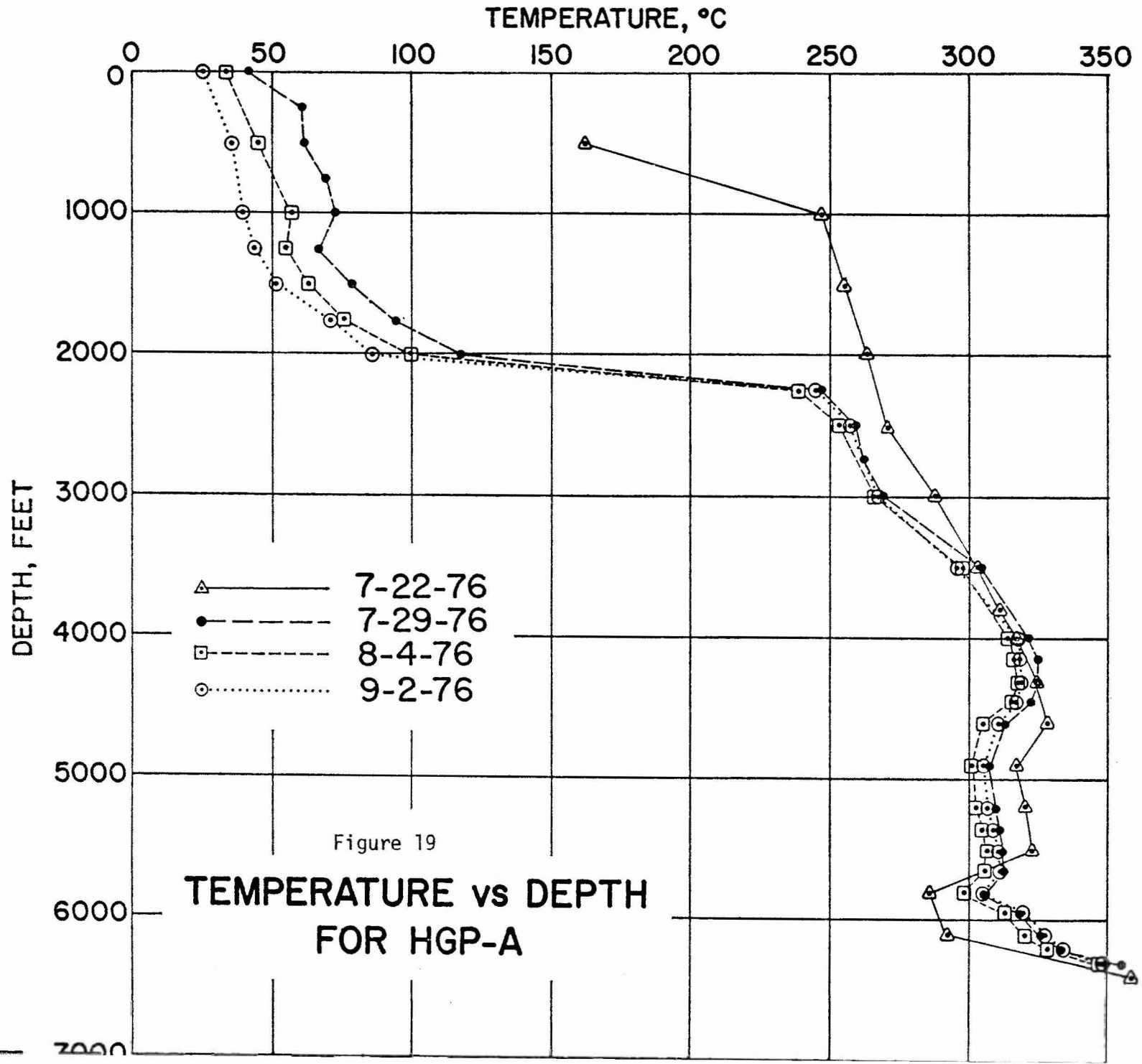

Figure 19

TEMPERATURE vs DEPTH FOR HGP-A

Eq. (8) can be rewritten in dimensionless form as

$$\frac{Nu_x}{Ra_x^{1/2}} = 0.444 \quad , \tag{9}$$

where $Nu_x \equiv \frac{hx}{k}$ and $Ra_x \equiv \rho_\infty g\beta K(T_w-T_\infty)x/\mu\alpha$ are the local Nusselt number and Rayleigh number. The temperature and vertical velocity distribution in the porous layer adjacent to an isothermal dike at 200°C in an aquifer at 15°C are shown in Figure 20.

Free Convection from a Cylindrical Shape Intrusive [15]. The problem of free convection about the outer surface of a vertical cylindrical intrusive with wall temperature $T_w = T_\infty + Ax^\lambda$ was treated by Minkowycz and Cheng [11] using local-similarity and local non-similarity methods. Figure 21 shows that the ratio of local surface heat flux for a cylindrical shape body with radius r_o to that of a flat plate with a width $S = 2\pi r_o$ depends on both λ (wall temperature distribution) and ξ where $\xi \equiv \frac{2x}{r_o} \frac{1}{(Ra_x)^{1/2}}$ is a measure of curvature effect.

Injection of Hot Water or Withdrawal of Cold Water Along Wells or Fissures [13]. For the special cases where the temperature and velocity of the mass flux are of the form $T_w = T_\infty \pm Ax^\lambda$ and $v = ax^n$, similarity solutions have been obtained for the special cases where $n = (\lambda-1)/2$. The effects of mass flux on the thermal boundary layer thickness and the temperature gradients at the wall for injection of hot water were investigated [13].

Mixed Convection About Vertical or Nearly Vertical Dikes [18]. For mixed convection about nearly vertical impermeable surfaces at a prescribed temperature $T_w = T_\infty + Ax^\lambda$, inclined at an angle $m\pi/2$ with respect to the horizon, and with free stream velocity $U = Bx^n$ where $n = m/(2-m)$, similarity solutions exist if $n = \lambda$.

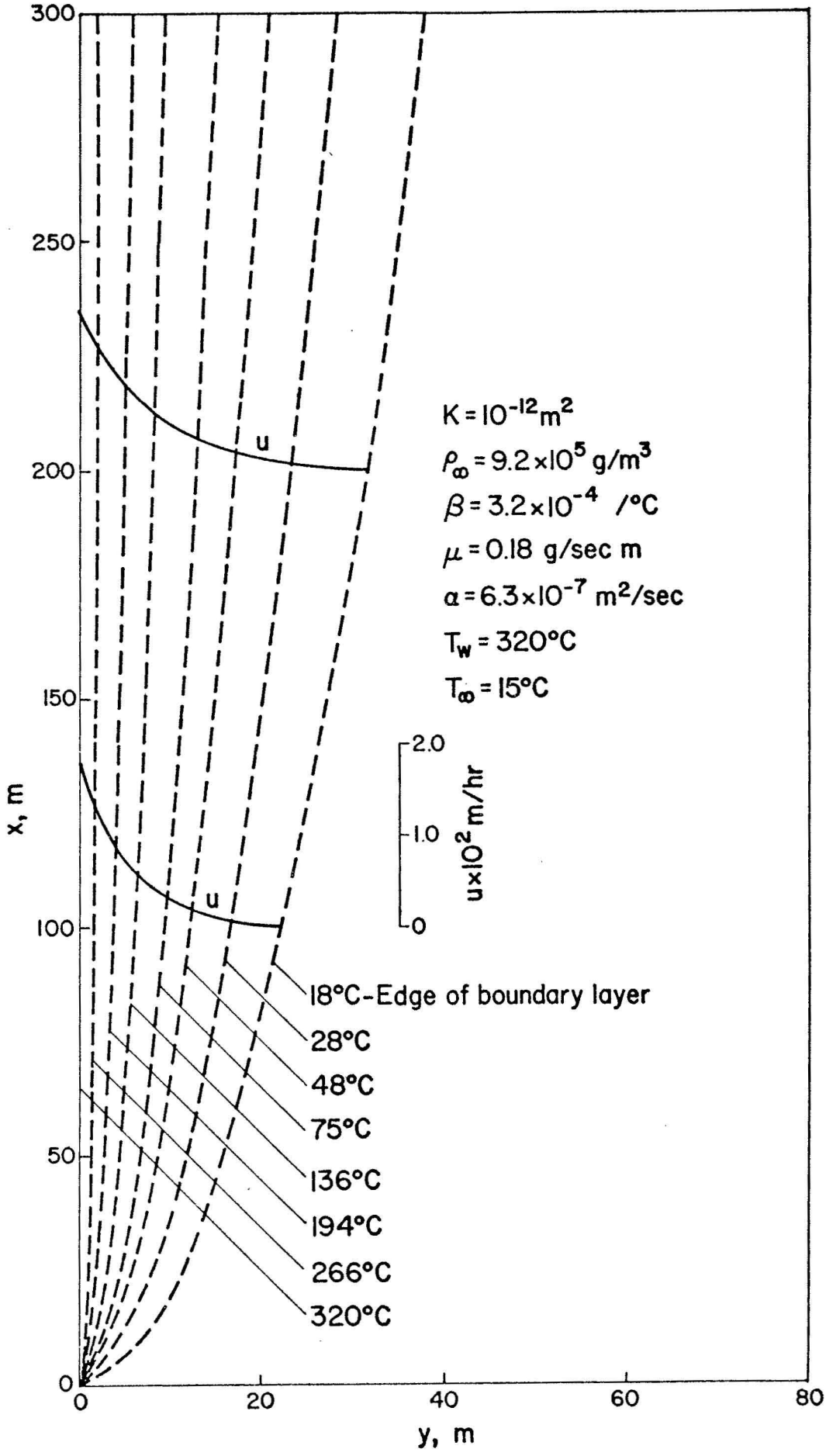

Figure 20. Isotherms and Velocity Distribution for a Dike with Uniform Wall Temperature

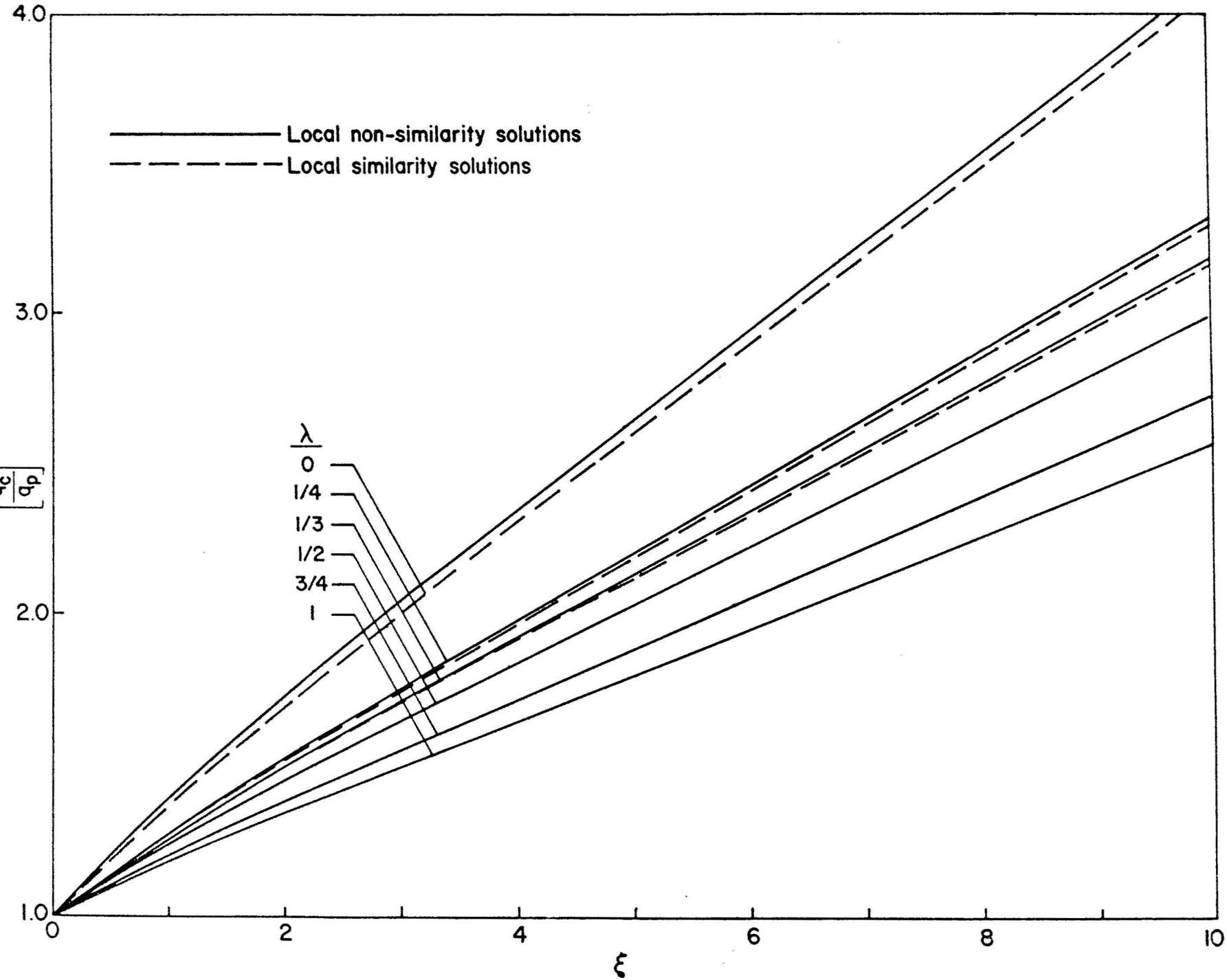

Figure 21. Local Surface Heat Transfer Ratio for Selected Values of λ

It is found that the thermal boundary layer thickness is

$$\frac{\delta_T}{x} = \frac{\eta_T}{\sqrt{RePr}} \quad , \tag{10}$$

and the surface heat flux is

$$q = kA \sqrt{\frac{\beta}{\alpha}} x \frac{3\lambda-1}{2} \left[-\theta'(0)\right] \quad , \tag{11}$$

which can be rewritten as

$$\frac{Nu}{\sqrt{RePr}} = -[\theta'(0)] \tag{12}$$

where $RePr = \frac{U_\infty x}{\alpha}$ and the values of η_T and $[-\theta'(0)]$ at different values of the prescribed parameter of Gr/Pe are shown in Figs. 22 and 23.

To gain some feeling on the order of magnitude of various physical quantities in a geothermal reservoir, consider a vertical heated surface (such as a dike) at 215°C embedded in an aquifer at 15°C. If a pressure gradient exists in the reservoir such that groundwater is flowing vertically upward with velocity U_∞, the values of heat transfer rate and the size of the hot water zone can be determined from Figs. 22 and 23. The results of the computations for U_∞ varying from 0.01 cm/hr to 10 cm/hr are plotted in Figs. 24 and 25. It is shown that the total heat transfer rate for a vertical heated surface, 1 km by 1 km, increases from 20 MW to 110 MW, while the thickness of the hot water zone at 1 km decreases from 130 m to 20 m.

Free & Mixed Convection About a Sill or Bedrock (12, 16)

Closed form solutions were obtained for free and mixed convection about a heated horizontal bedrock in an aquifer. Effects of cold water injection near a heated bedrock or a sill were also considered. It is found that the controlling parameter for the problem is the prescribed parameter $Ra/(RePr)^{3/2}$. The effects of this parameter to heat transfer rate and the size of hot water zone were also investigated (12, 16).

Unsteady Convective Heat Transfer and Effects of Non-isothermal Environment

The effects of unsteady convection and non-isothermal environment for free convection adjacent to hot intrusives were considered by Johnson and Cheng [21]. It is found that similarity solutions with non-isothermal environments exist only for steady free convection about vertical surfaces. Also, several very specific solutions exist for unsteady free convection about vertical and horizontal heated surfaces and vertical cylindrical shape intrusives.

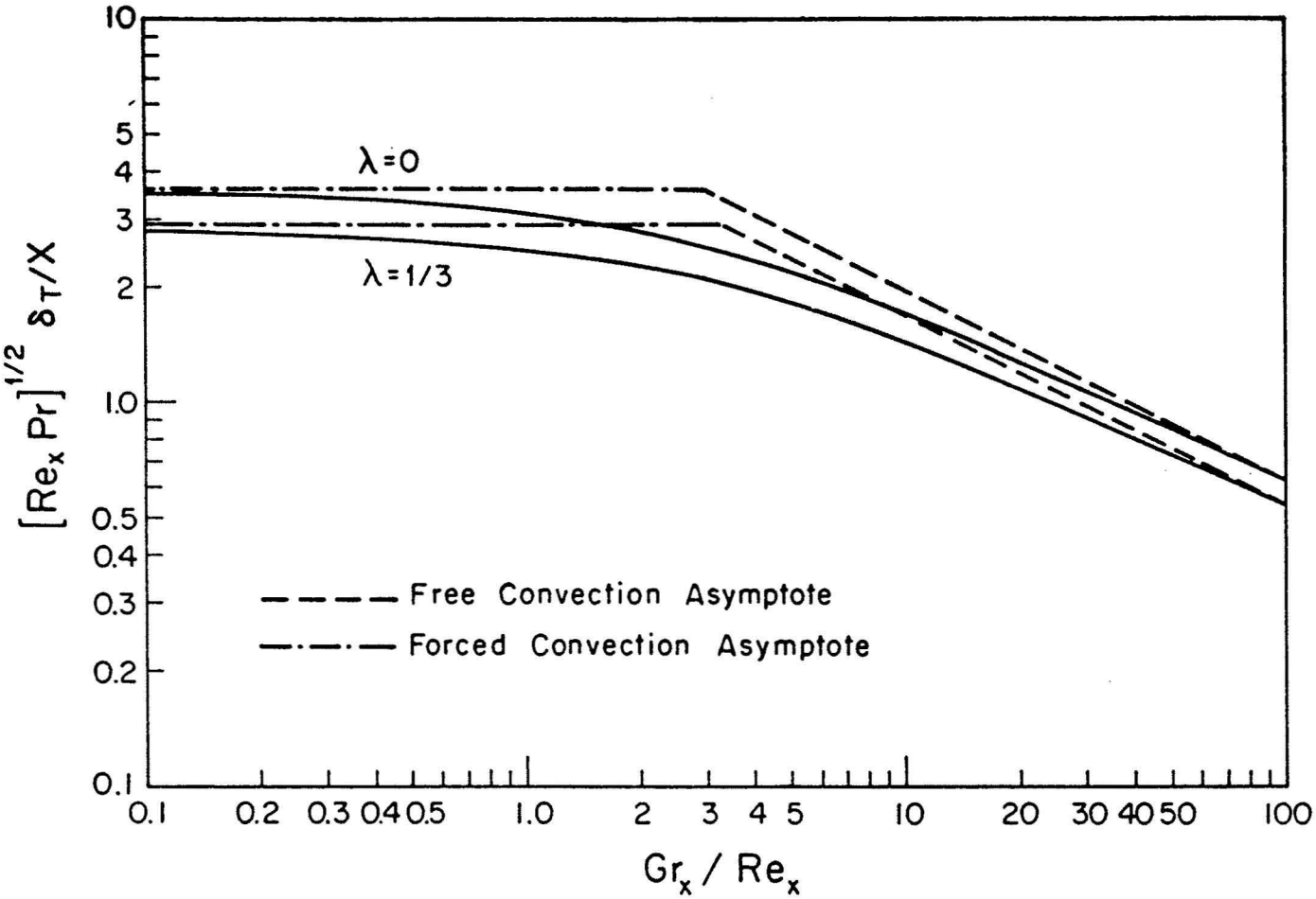

Figure 22. Dimensionless Boundary Layer Thickness Parameter for Aiding Flows about a Dike

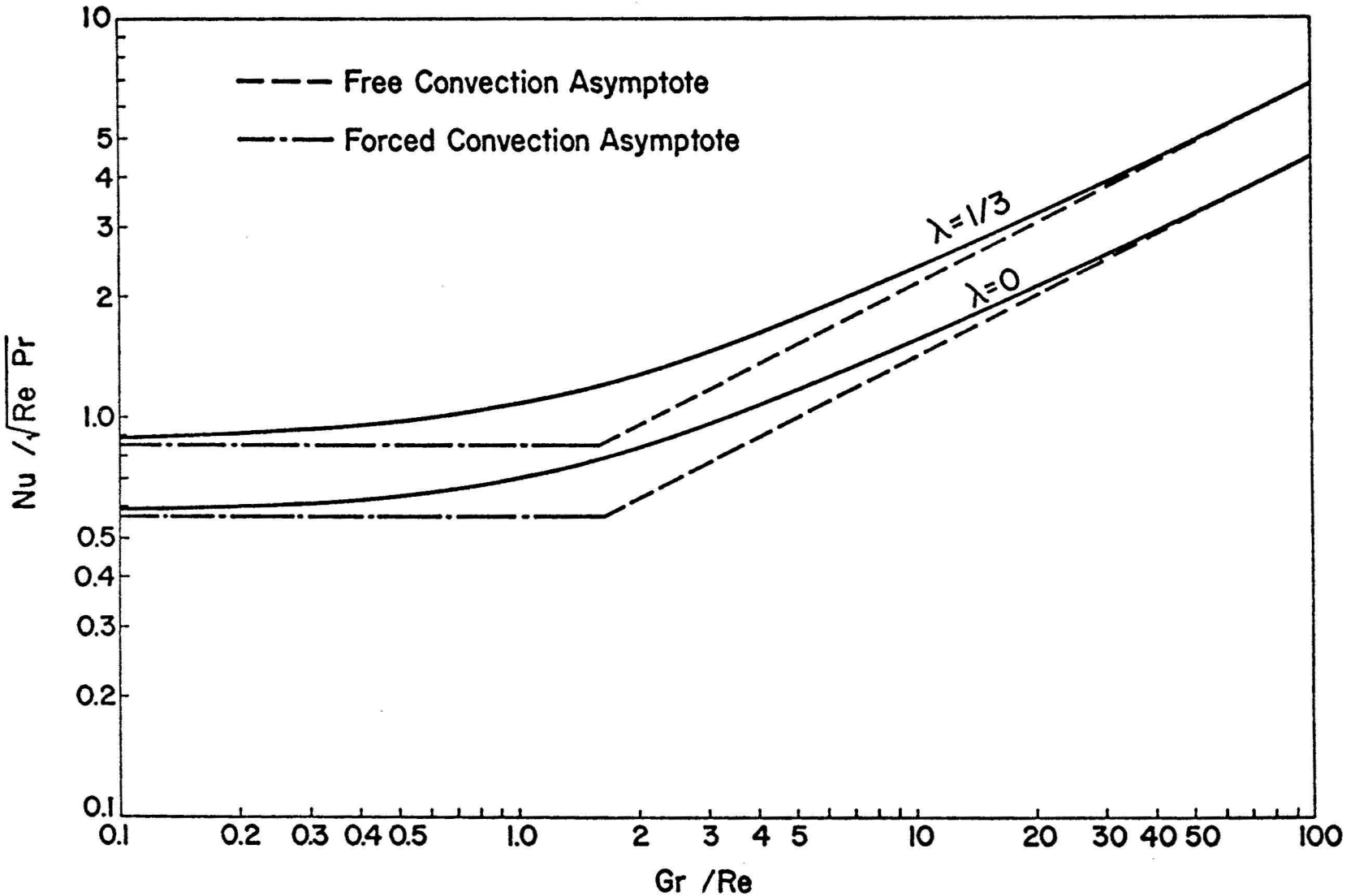

Figure 23. Heat Transfer Results for Aiding Flows about a Dike

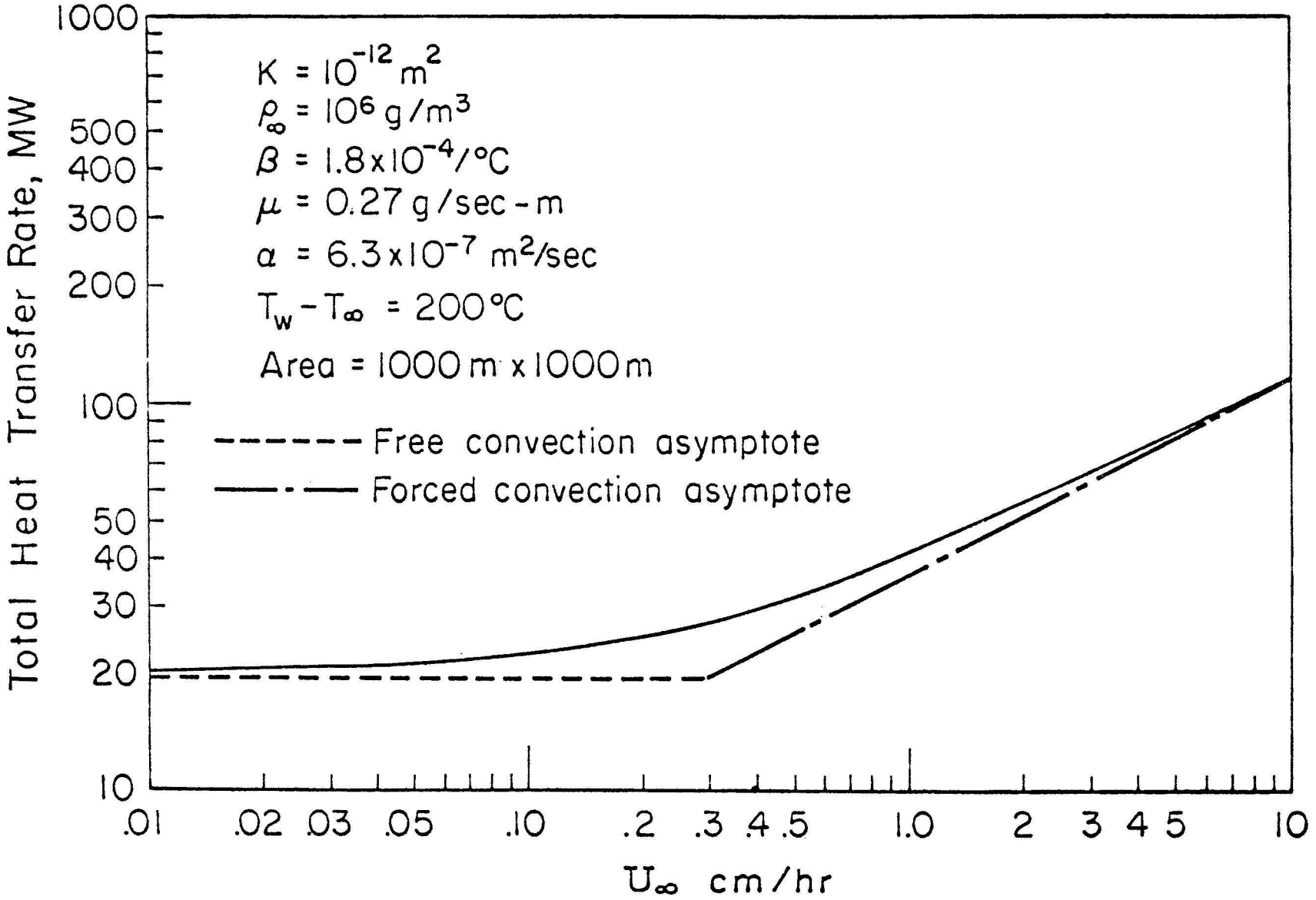

Figure 24. The Effect of U_∞ on Total Heat Transfer Rate for Mixed Convection from an Isothermal Dike in a Volcanic Geothermal Reservoir

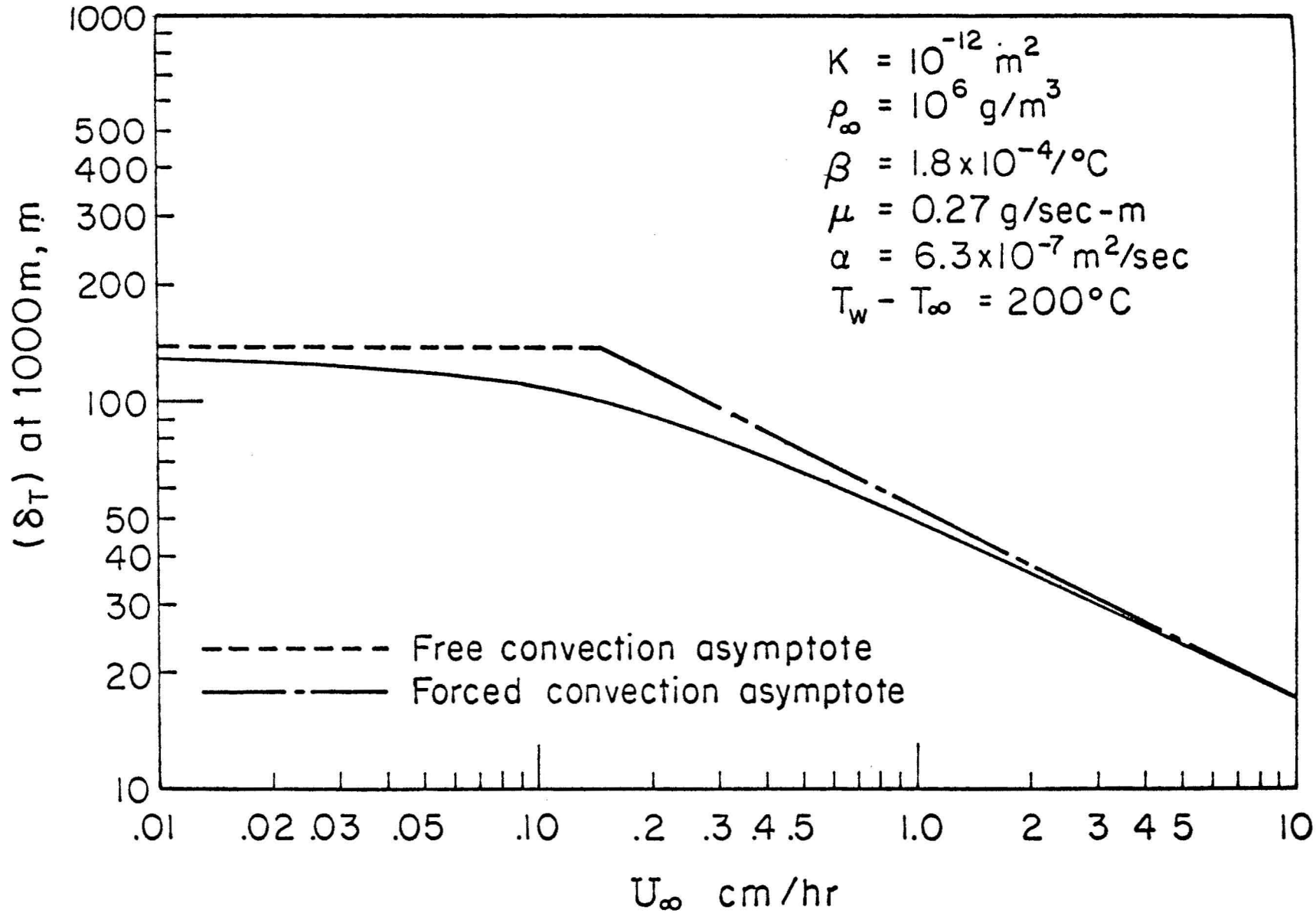

Figure 25. The Effect of U_∞ on the Size of Hot Water Zone for Mixed Convection from a Vertical Isothermal Dike in a Volcanic Geothermal Reservoir

Integral Methods for Convective Heat Transfer in Rock Formation

The Karman-Pohlhausen integral method, widely used in classical convective heat transfer problems, has also been investigated for possible application to convective heat transfer problems in a subsurface formation [22]. To check the accuracy of the approximate method, the problems of free and mixed convection adjacent dikes and sills where similarity solutions have been obtained are solved on the basis of the integral method. It is found that the results for Nusselt numbers based on integral methods are in good agreement with those obtained from similarity solutions. Thus, the integral methods can be applied with confidence to other convective heat transfer problems in subsurface environment where no similarity solutions exist.

REFERENCES

1. Keller, G.V., "Drilling at the Summit of Kilauea Volcano," prepared for N.S.F., Colorado School of Mines, March 1974.

2. Shito, S., "Warm Water Wells on the Island of Hawaii", TM #1, Jan. 1974.

3. Cheng, P., & Lau, K.H., "Steady State Free Convection in an Unconfined Geothermal Reservoir," J.G.R., V. 79, 4425-4431 (1974).

4. Lau, K.H., & Chen, P., "The Effect of Dike Intrusion on Free Convection in Unconfined Geothermal Reservoirs," Int. J. Heat & Mass Transfer, V. 20, 1205 - 1210 (1977).

5. Cheng, P. Yeung, K.C., and Lau, K.H., "Numerical Solution for Steady Free Convection in Confined Geothermal Reservoirs," Proceedings of 1975 International Seminar on Future Energy Production, edited by N. Afgan and J.P. Hartnett, 429-448, Hemisphere Publishing Co., (1975).

6. Cheng, P. and Lau, K.H., "The Effect of Steady Withdrawal of Fluid in Confined Geothermal Reservoirs," Proceedings of the Second United Nations Symposium on the Development and Use of Geothermal Resources, 1591-1598 (1977).

7. Cheng, P, "Numerical and Analytical Studies on Heat and Mass Transfer in Volcanic Island Geothermal Reservoirs," Proceedings of 1st Workshop on Geothermal Reservoir Engineering and Well Stimulation, 219-224 (1975), Stanford University, Stanford, California.

8. Cheng, P., and Lau, K.H., "Modelling of Hawaii Geothermal Resources," Geothermics, V. 2, 90-93 (1976).

9. Cheng, P., and Teckchandani, L., "Transient Heating and Withdrawal of Fluids in Geothermal Reservoirs," The Earth's Crust, A.G.U. Momograph No. 20, 705-736 (1977).

10. Rana, R., Horne, R.N., & Cheng, P., "Numerical Solutions for Free Convection in a Multi-Layered Geothermal Reservoir," to appear in J. of Heat Transfer (1978).

11. Cheng, P., & Minkowycz, W.J., "Free Convection About a Vertical Flat Plate Embedded in a Porous Medium with Application to Heat Transfer from a Dike," by J. Geophysical Research, V. 82, No. 14, 2040-2044 (1977).

12. Cheng, P., and Chang, I-Dee, "Buoyancy Induced Flows in a Porous Medium Adjacent to Impermeable Horizontal Surfaces," Int. J. of Heat & Mass Transfer, V. 19, 1267-1272 (1976).

13. Cheng, P., "The Influence of Lateral Mass Flux on Free Convection Boundary Layers in a Saturated Porous Medium," Int. J. Heat & Mass Transfer, V. 20, 201-206 (1977).

14. Cheng, P., "Heat and Mass Transfer in Liquid-Dominated Geothermal Reservoirs," Letters in Heat & Mass Transfer, V. 3, 81-88 (1976).

15. Minkowycz, W.J., and Cheng, P., "Free Convection About a Vertical Cylinder Embedded in a Porous Medium," Int. J. of Heat & Mass Transfer, V. 19, 805-813 (1976).

16. Cheng, P., "Similarity Solutions for Mixed Convection from Horizontal Impermeable Surfaces in Saturated Porous Media," Int. J. of Heat Mass Transfer, V. 20, 893-898 (1977).

17. Cheng, P., "Constant Surface Heat Flux Solution for Porous Layer Flows," Letters in Heat & Mass Transfer, V. 4, 119-128 (1977).

18. Cheng, P., "Combined Free and Forced Boundary Layer Flows About Inclined Surfaces in a Porous Medium," Int. J. Heat Mass Transfer, V. 20, 807-814 (1977).

19. Cheng, P., "Buoyancy Induced Boundary Layer Flows in Geothermal Reservoirs," presented at the 2nd NSF Workshop on Geothermal Reservoir Engineering, December 1-3, 1976, Stanford University, Stanford, California.

20. Cheng, P., & Chau, W.C., "Similarity Solutions for Convection of Groundwater Adjacent to Horizontal Impermeable Surface with Axisymmetric Temperature Distribution", Water Resources Research, V. 13, 768-772 (1977).

21. Johnson, C.H., and Cheng, P., "Possible Similarity Solutions for Free Convection Boundary Layers Adjacent to Flat Plates in Porous Media,", Int. J. Heat Mass Transfer, V. 21, 709-718 (1978).

22. Cheng, P., "Convective Heat Transfer in Porous Layers by Integral Methods," Letters in Heat and Mass Transfer, 1978, V. 5, 243-252.